SRNL-STI-2009-00810
Rev. 0

PERFORMANCE PROPERTIES OF SALTSTONE PRODUCED USING SWPF SIMULANTS

J. R. Harbour and T. B Edwards

Savannah River National Laboratory

December 2009

Savannah River National Laboratory
Savannah River Nuclear Solutions
Aiken, SC 29808

Prepared for the U.S. Department of Energy Under Contract Number DE-AC09-08SR22470

SRNL
SAVANNAH RIVER NATIONAL LABORATORY

DISCLAIMER

Printed in the United States of America

Prepared For
U.S. Department of Energy

SRNL-STI-2009-00810
Rev. 0

Key Words: *Curing Temperature*
Porosity
Young's Modulus

Retention: Permanent

PERFORMANCE PROPERTIES OF SALTSTONE PRODUCED USING SWPF SIMULANTS

J. R. Harbour and T. B Edwards

Savannah River National Laboratory

December 2009

Savannah River National Laboratory
Savannah River Nuclear Solutions
Aiken, SC 29808

Prepared for the U.S. Department of Energy Under Contract Number DE-AC09-08SR22470

REVIEWS AND APPROVALS

AUTHORS:

J. R. Harbour, SRNL, Engineering Process Development Date

T. B. Edwards, SRNL, Applied Comp Eng & Statistics Date

TECHNICAL REVIEWERS:

M. M. Reigel, SRNL, Engineering Process Development Date

APPROVERS

A. B. Barnes, SRNL, Manager, Engineering Process Development Date

S. L. Marra, SRNL, Manager, E&CPT Research Programs Date

J. E. Occhipinti, Manager, Waste Solidification Engineering Date

EXECUTIVE SUMMARY

The overwhelming majority of waste to be immobilized at the Saltstone Production Facility will come from the waste stream exiting the Salt Waste Processing Facility (SWPF). These SWPF batches are salt solutions that result from pretreatment of the High Level Waste (HLW) supernate by an Actinide Removal Process followed by Caustic Side Solvent Extraction. The concentration of aluminate within these streams will vary and be determined by (1) the concentration in the incoming salt waste stream, (2) the degree of aluminum leaching from the HLW, (3) the method for introducing the aluminate into the waste stream (continuous or batch) and (4) and any operational or regulatory limitations.

The overall Performance Assessment outcome for the Saltstone Disposal Facility will depend significantly on the performance properties of the SWPF Saltstone grouts. This report identifies and quantifies, when possible, those factors that drive the performance properties of the projected SWPF grouts [1]. Previous work has identified aluminate concentration in the salt waste stream as a key factor in determining performance [2]. Consequently, significant variation in the aluminate concentration to a maximum level of 0.65 M was investigated in this report. The SWPF baseline grout is a mix with a 0.60 water to cementitious ratio and a premix composition of 45 wt % slag, 45 wt % fly ash and 10 wt % portland cement.

The key factors that drive performance of the SWPF mixes were determined to be (1) the time/temperature profile for curing, (2) water to cementitious materials ratio, (3) aluminate concentration in the waste stream, and (4) wt % slag in the premix.

An increase in the curing temperature for mixes with 45 wt % slag resulted in a 2.5 times decrease in Young's modulus. The reduction of Young's modulus measured at 60 °C versus 22 °C was mitigated by an increase in the aluminate concentration but was still significant. For mixes containing 60 wt % slag, the reduction in Young's modulus between these two curing temperatures was significantly lessened. The importance of curing conditions can not be overemphasized. The gain realized in performance by, e.g., a higher level of aluminate or wt % slag or a reduction in w/cm ratio, can be offset by the effects of a higher curing temperature. In fact, the final performance properties of a mix cured at 60 °C can be lower than the initial values before any of the performance enhancing changes are introduced. Control of the time/temperature curing profile can be managed by pour schedules and other temperature control measures.

The reduction in performance at higher curing temperatures is consistent with results obtained in a separate study [3]. Although preliminary, results from this task on the measurement of hydraulic conductivity at MACTEC showed that curing of a Saltstone mix at 60 °C increased the hydraulic conductivity by several orders of magnitude [1]. The permeability data are based on only one mix but, were consistent with a measured reduction in Young's modulus for these same samples. Therefore, it is recommended that impact of curing temperature on performance properties be further investigated.

An increase in dynamic Young's modulus (indicator of performance) is observed as the water to cementitious materials (w/cm) ratio decreases. The w/cm ratio is a process parameter which can

be adjusted to improve performance as long as the processing properties of the grout are still within an operational window that will lead to successful placement. The same conclusions apply to wt % slag in the premix. That is, an increase in the wt % slag at the expense of fly ash in the premix increases Young's modulus and performance. An increase in wt % slag (as with a decrease in w/cm ratio) increases viscosity and yield stress and a final mix design must be balanced such that acceptable processing properties are obtained.

The performance properties of SWPF mixes show a non-linear dependence on aluminate concentration. As the aluminate concentration is increased from 0.1 M to 0.25 M, the Young's modulus and compressive strength increase and the porosity is reduced. Consistent with this improvement in performance is an increase in the heat of hydration, reflective of an increase in the degree of hydration. Higher degrees of hydration in mixes generally lead to better performance. In the region of 0.25 to 0.45 M aluminate, very little additional change is observed in any of the properties. A further increase in the aluminate concentration from 0.45 M to 0.65 M leads to a slight reduction in Young's modulus. It was observed however, that the values of Young's modulus for samples cured at 22 °C decreased after approximately 50 days. This was the first time a reduction in Young's modulus was observed as a function of time and is most likely correlated with the high levels of aluminate present in these mixes. This reduction can be accounted for by cracking of the Saltstone samples with time. Further work will be required to fully identify the cause of this reduction in Young's modulus.

A simple method was developed and is discussed in this report which reflects general trends in permeability of the cured grout samples as a function of curing temperature. This method reveals that curing at higher temperatures (e.g., 60 °C) results in a microstructure that is different than the microstructure observed for the same mixes cured at 22 °C. Furthermore, the microstructure observed at 60 °C for these SWPF mixes containing normal premix, is similar to that observed for the Saltstone mix cured at 60 °C with the very high permeability measured at MACTEC. Measurements of the heat of hydration at 50 °C reveal that in certain cases, the degree of hydration is also reduced by curing at higher temperatures. Thus, it appears that curing Saltstone at higher temperatures from waste streams containing aluminate concentrations of 0.25 M or higher, reduces the degree of hydration and transforms the microstructure of the final waste form.

Linear, empirical models were developed and are presented in this report for Young's modulus, heat of hydration normalized to the mass of premix, heat of hydration normalized to the mass of grout, yield stress and plastic viscosity. The models included only data from the mixes batched as part of Phases 9 and 12. Therefore, the models quantify the statistically significant factors that drive the performance and processing properties over the ranges selected in the designs for Phases 9 and 12. The R^2 values for these three models ranged from 93% to 99%.

The final performance properties of SWPF mixes are dependent upon a number of interactive factors in a complex fashion. Depending upon the values of the performance properties that are required to meet the Performance Assessment, these factors may need to be controlled to achieve the desired outcome.

TABLE OF CONTENTS

LIST OF FIGURES

LIST OF TABLES

LIST OF ACRONYMS

ACTL	Aiken County Technology Laboratory
ARP	Actinide Removal Process
CBO	Carbon Burn-Out
CSH	Calcium Silicate Hydrate
E	Young's Modulus
FA	Class F Fly Ash
BFS	Blast Furnace Slag
DSS	Decontaminated Salt Solution
GPa	Giga Pascals
GVS	Grout Variability Study
HLW	High Level Waste
HOH	Heat of Hydration
M	Molarity
MCU	Modular Caustic Side Solvent Extraction
Φ	Total Porosity
PA	Performance Assessment
PC	Portland Cement
SDF	Saltstone Disposal Facility
SPF	Saltstone Production Facility
SRNL	Savannah River National Laboratory
SRNS	Savannah River Nuclear Solutions
SRS	Savannah River Site
SWPF	Salt Waste Processing Facility
T	Temperature
TR	Trial Run
w/cm	Water to Cementitious Material Ratio
Wt	Weight
Wt %	Weight Percent

1.0 INTRODUCTION

At the Saltstone Production Facility (SPF), decontaminated salt solution (DSS) is combined with premix (a cementitious mixture of portland cement (PC), blast furnace slag (BFS) and Class F fly ash (FA)) in a Readco continuous mixer to produce fresh (uncured) Saltstone. After transfer to the Saltstone Disposal Facility (SDF), the hydration reactions initiated during the contact of the premix and salt solution continue during the curing period (typically months) to produce the hardened waste form product. The amount of heat generated from hydration and the resultant temperature increase in the vaults depend on the composition of the decontaminated salt solution being treated as well as the grout formulation (mix design). Curing the Saltstone at temperatures present in the disposal vaults turns out to play an important role in determining the performance properties of the Saltstone.

Most of the waste to be immobilized at the Saltstone Production Facility will come from the waste stream exiting the Salt Waste Processing Facility (SWPF). These SWPF batches are salt solutions resulting from pretreatment of the High Level Waste (HLW) supernate by an Actinide Removal Process followed by Caustic Side Solvent Extraction. This report focuses on Saltstone mixes batched using a simulant based on the average projected SWPF waste stream composition [1]. In particular, the focus will be on performance properties although processing properties will also be presented.

The overall Performance Assessment outcome for Saltstone Disposal Facility will depend on the performance properties of the SWPF Saltstone grouts. This report identifies and quantifies, when possible, those factors that drive the performance properties of the projected SWPF grouts. Previous work has identified aluminate concentration in the salt waste stream as a key factor in determining performance and consequently, a significant variation in the aluminate concentration (from 0.35 to 0.65 M in Phase 12) was investigated in this report [2-4].

The performance properties of the cured Saltstone depend in part on the degree of hydration of the cementitious materials that make up the premix. The degree of hydration can be estimated by measurement of the heat of hydration through isothermal calorimetry. It turns out that a higher degree of hydration, as reflected by higher heat of hydration, leads to a better product in terms of performance [4]. Therefore, there are competing effects between lowering the heat of hydration in order to reduce the associated temperature increase in the vault and improving the performance properties through higher heats of hydration.

The role of curing temperature on performance properties is significant in Saltstone mixes and in order to investigate the cause of this dependence, (1) heats of hydration were measured at elevated temperatures and (2) a method was developed and implemented that provided general insight into the microstructure and permeability of the grout as a function of curing temperature.

Empirical models were developed for Young's modulus, heat of hydration (normalized to premix and to mass of the grout), yield stress and plastic viscosity. These models provide insight into the drivers of these properties over the range of variation for the factors of this study.

2.0 EXPERIMENTAL

2.1 Materials

The cementitious materials were obtained from the SPF in five gallon containers and are listed in Table 2-1. These materials were specified in a contract for Saltstone cementitious materials and arrived with the delivery of the cementitious materials to Saltstone. The materials were transferred to smaller high-density polyethylene bottles at Aiken County Technology Laboratory (ACTL) and the bottles were tightly sealed. Maintaining these materials in a tightly sealed container limits the exposure of the materials to humid air and hydration prior to use. Table 2-1 also contains the wt% contribution of each material used to make the nominal premix. The fly ash used in this study was a material that had been thermally treated by the vendor to remove most of the carbon and ammonia (carbon burnout or CBO fly ash).

Table 2-1. Saltstone Cementitious Materials and Current Premix Blend.

Material	Category	Vendor	Premix Blend (wt%)
Portland Cement	Type II	Holcim	10
Blast Furnace slag	Grade I	Holcim	45
Fly Ash	Class F	SEFA	45

The SWPF simulant was an average composition based on projections of SWPF batches [4] and the baseline composition is provided in Table 2-2.

Table 2-2. Baseline SWPF Simulant at 0.350 Aluminate Concentration.

BATCH SHEET FOR SWPF SIMULANT			
	TARGET		REFERENCE
Compound	Molarity	MW	Amt / Liter
	Moles/Liter	grams/mole	grams
50% by Weight NaOH	3.809	40.00	**304.69**
$NaNO_3$	0.923	84.99	**78.45**
$NaNO_2$	0.485	68.99	**33.43**
Na_2CO_3	0.118	105.99	**12.46**
Na_2SO_4	0.055	142.04	**7.84**
Aluminum Nitrate (9 H2O)	0.350	375.13	**131.30**
Sodium Phosphate (12 H2O)	0.007	380.12	**2.76**
Total Salt mass			360.31
Total Na Molarity	5.58		

Free Hydroxide	**2.41**
Final $NaNO_3$	**1.97**
Total NO_3 plus NO_2	**2.46**

2.2 Experimental Design

The mixes in this study were prepared under Phase 12 of the Saltstone Variability Study. Some of the results from Phase 9 of the SWPF variability study were integrated into the results of Phase 12 for the predictive modeling. The design for Phase 12 is presented in Section 3.0 of this report.

2.3 Measurement of Properties

The measurements of heat of hydration [5], dynamic Young's modulus [6], porosity [7], and processing properties such as set time [8] were performed by the methods described previously.

2.4 Curing at Higher Temperatures

Samples were cured at ambient conditions in the laboratory (nominally 22 °C) and at 40 °C, 60 °C, or 75 °C. In all cases the grout was poured into the cylinders, capped and securely taped. Measurements of the mass of the samples with container, lid and tape were made prior to and after curing to measure any mass loss during curing. At ambient temperature and at 40 °C curing conditions, essentially no change in the mass after curing was noted. For the 60 °C curing conditions, a mass loss on the order of 1 to 2 grams was observed. For example, the Young's modulus cylinder and sample have a starting mass of ~ 1100 grams. Therefore, a loss of 1 gram corresponds to only ~ 0.1 wt % of the total mass of the sample.

The ovens have temperature gradients within the interior of the ovens. Therefore, the range of temperatures for a given sample may be as great as ± 5 °C about a set temperature. Thermocouples and thermometers were used to measure the actual temperatures within the oven.

3.0 RESULTS AND DISCUSSION

The results presented in this report were generated as part of Task 4 of the Saltstone Variability Study for FY09 with a focus on the dependence of performance properties on factors including wt % slag, aluminate concentration and temperature of curing [1]. The simulants used in this task were based on previous projections of the SWPF batches in order to be consistent with previous phases of the Variability Study. An experimental design for Phase 12 was developed and is presented in Table 3-1. Results of SWPF mixes from Phase 9 were also included for some of the analyses [9].

Table 3-1. Experimental Design for Phase 12.

	SWPF Grout Variability Study Phase 12 Aluminate									
Run Number	Temp	Water/Premix	OPC	FA	Slag	Added OH	Free OH	Nitrate plus Nitrite	Phosphate	Aluminate
Run Order	°C	Ratio	Wt %	Wt %	Wt %	Molarity	Molarity	Molarity	Molarity	Molarity
GVS121	22	0.60	10	45	45	3.81	2.41	2.457	0.0073	0.35
GVS122	22	0.60	10	45	45	4.21	2.41	2.457	0.0073	0.45
GVS123	22	0.60	10	45	45	4.61	2.41	2.457	0.0073	0.55
GVS124	22	0.60	10	45	45	5.01	2.41	2.457	0.0073	0.65
GVS125	22	0.60	10	30	60	3.81	2.41	2.457	0.0073	0.35
GVS126	22	0.60	10	30	60	4.21	2.41	2.457	0.0073	0.45
GVS127	22	0.60	10	30	60	4.61	2.41	2.457	0.0073	0.55
GVS128	22	0.60	10	30	60	5.01	2.41	2.457	0.0073	0.65

3.1 Degree of Hydration

It is clear from the results of previous phases of the Saltstone Variability Study that the degree of hydration is a major determining factor in the performance properties of the Saltstone mixes. Specifically, as the degree of hydration increases, the compressive strength, Young's modulus, and permeability also increase while the porosity decreases.

One method for determining the degree of hydration is through the measurement of heat of hydration. For example, a portland cement and water mix at a 0.60 water to cement ratio generates approximately 400 J/g of cement after curing for 28 days. This is close to the maximum amount of heat that is released through hydration if 100% of the cement hydrates. Therefore, in this example the degree of hydration of the portland cement in water is close to 100%.

For the mixes of Phase 12, a comparison was made between the projected and actual degrees of hydration. The projections were estimated by first measuring the heat of hydration released from mixes batched according to the design mix of GVS123 except that in one mix 100% slag was used, in a second mix 100% cement was used, and in the third mix 100% fly ash was used instead of the normal premix (see Figures 3-1 through 3-3). Since heat of hydration is time dependent, values for these three mixes were measured after 41 days for the point of comparison. These values were then used with the simple law of mixtures to predict the heat of hydration using blended premixes.

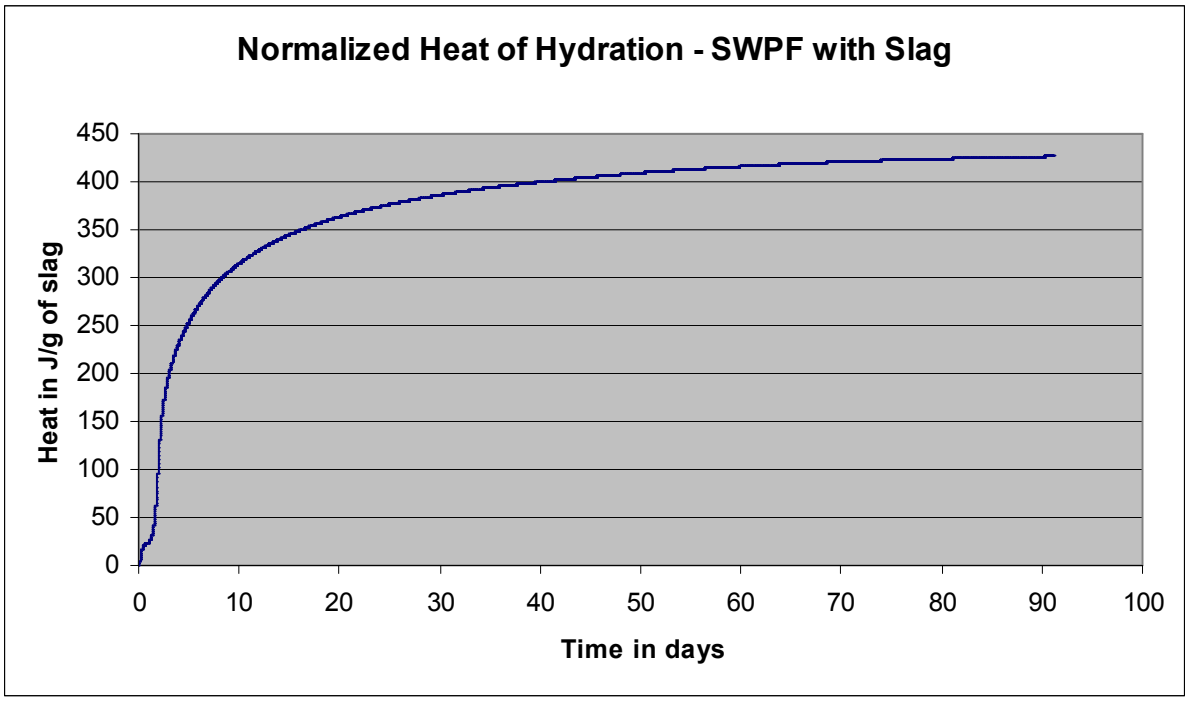

Figure 3-1. Normalized heat of hydration for an SWPF mix design (GVS123) using slag only.

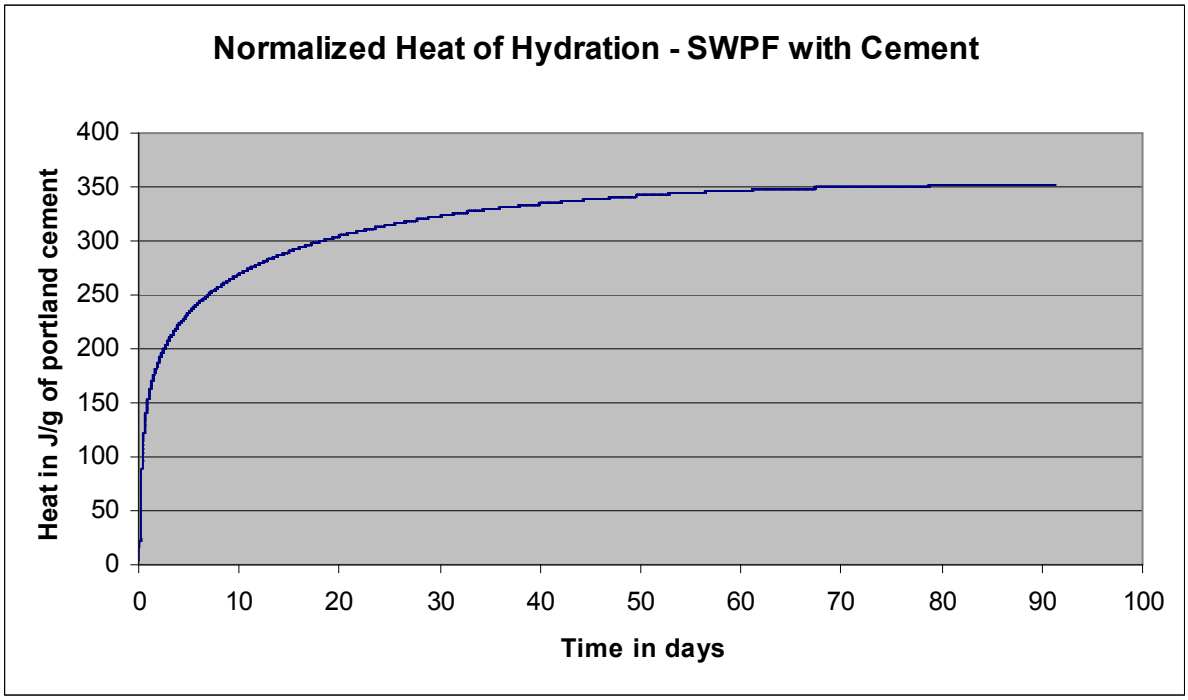

Figure 3-2. Normalized heat of hydration for an SWPF mix design (GVS123) using cement only.

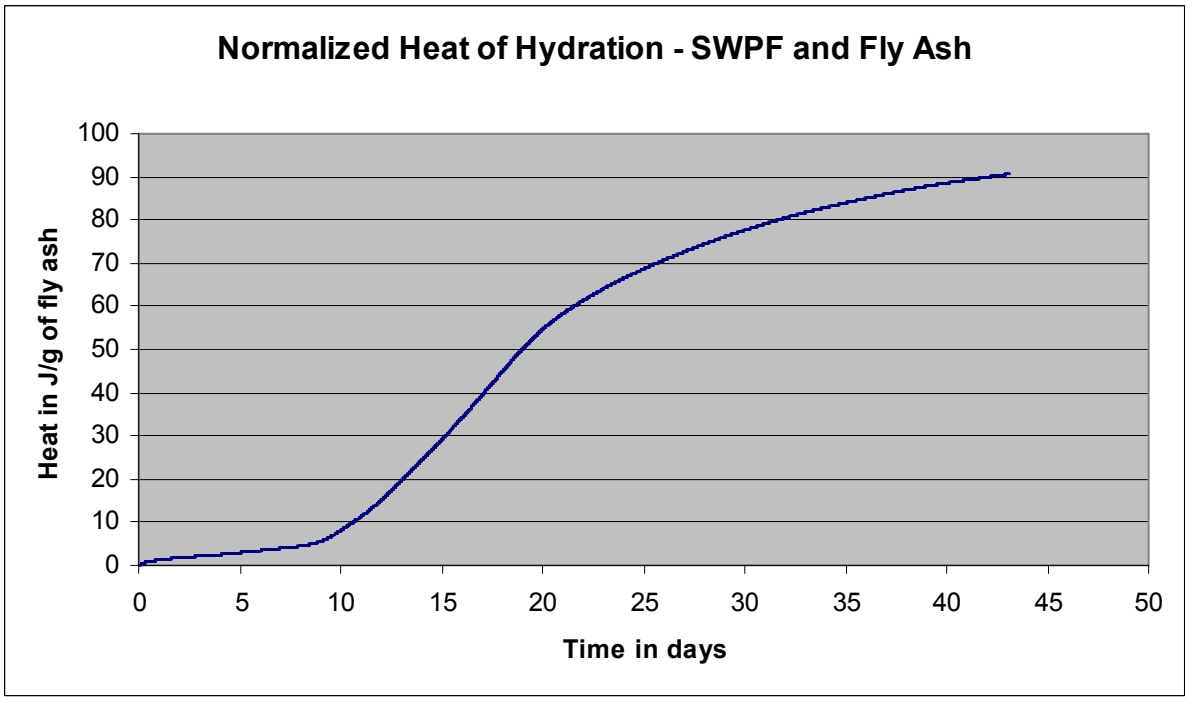

Figure 3-3. Normalized heat of hydration for an SWPF mix design (GVS123) using fly ash only.

Using the simple law of mixtures and the experimental values of heat generation for the individual cementitious materials in the GVS123 mix, the projected heats of hydration were

calculated. These projected values along with the measured heat values are provided in Table 3-2. A comparison of the projected and measured values shows that the projected heat values were very close to the measured values for the mixes containing 60 wt % slag whereas the predicted values for the 45 wt % slag mixes were slightly higher than the measured values. To first order, the predicted values of heat production are consistent with the measured values of heat of hydration reflecting that there are no interactions between the premix components in this salt solution that limit hydration.

However, for SWPF or ARP/MCU mixes with relatively low aluminate levels (< 0.11 M), there is a relatively large difference between the measured and predicted heats of hydration. For example, an SWPF mix with the normal premix distribution and a relatively low aluminate concentration of 0.114 M had a heat of hydration of 175 J/g (corrected for the use of beneficiated fly ash) [4, 9]. The predicted value was 247 J/g for this duration of hydration, and therefore, the degree of hydration for this mix at a lower aluminate level is 71%. The degree of hydration is calculated by dividing the measured heat of hydration by the predicted heat of hydration.

A second example is a mix batched using an ARP/MCU simulant containing 0.05 M aluminate with a measured heat of hydration of 140 J/g compared to a predicted value of 210 J/g [10]. Therefore, the degree of hydration for this ARP/MCU mix was 67%. However, a mix batched using the ARP/MCU simulant with 0.28 M aluminate had a heat of hydration value of 210 J/g over the same time period, essentially equivalent to the predicted value (100% degree of hydration).

Table 3-2. Measured Versus Predicted Values for the Heat of Hydration of the Phase 12 Mixes.

	slag	cement	fly ash	Measured Heat		Predicted Heat
	wt %	wt %	wt %	J/g of cm	days	J/g of cm
GVS123	100	0	0	403	41	
GVS123	0	100	0	339	41	
GVS123	0	0	100	88	41	
GVS121	45	10	45	230	41	254
GVS122	45	10	45	237	41	254
GVS123	45	10	45	235	41	254
GVS124	45	10	45	239	41	254
GVS125	60	10	30	295	42	302
GVS126	60	10	30	297	42	302
GVS127	60	10	30	302	42	302
GVS128	60	10	30	299	42	302

The results from past and current testing show that mixes containing low levels of aluminate reach ~ 70% hydration whereas mixes containing higher levels of aluminate reach 100% hydration. This suggests, for mixes cured at 22 °C, that an aluminate concentration of ~0.25 M will lead to an increased degree of hydration and improved performance properties for Saltstone.

3.2 Young's Modulus

The impact of aluminate concentration on the Young's modulus (E) for samples cured at 22 °C over the aluminate range covered in the design for Phase 12 is shown in Table 3-3. Higher values of E (between 7 to 18%) were measured for the 4 samples containing the 60 wt % slag relative to the mixes containing the normal 45 wt % slag in the premix. The values of Young's modulus were relatively constant for mixes containing 0.35 or 0.45 M aluminate. However, as the aluminate concentration increased from 0.45 M to 0.55M through 0.65 M, the values of E decreased slightly. Figure 3-4 provides a plot of E vs. aluminate concentration for the 8 SWPF mixes of Phase 12.

Table 3-3. Young's Modulus Values for all Mixes Cured at 22 °C.

Mix Number	E (GPa)
	Cured at 22 °C
GVS121	9.8
GVS122	9.8
GVS123	9.0
GVS124	7.7
GVS125	10.5
GVS126	10.6
GVS127	10.3
GVS128	9.1

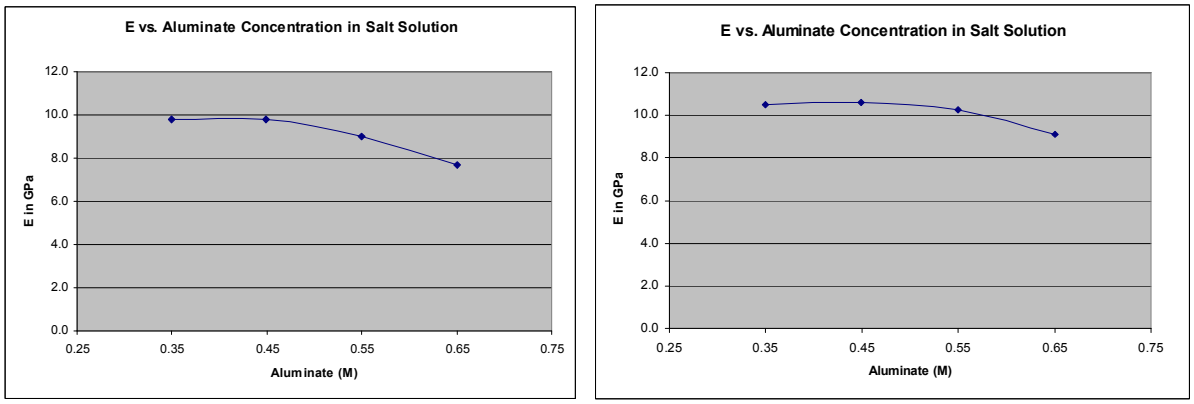

Figure 3-4. Plot of the data from Table 3-3. The figure on the left is for the GVS121-124 mixes while the figure on the right is for the GVS125-128 mixes.

Figures 3-5 and 3-6 show the time dependence of E for the 8 mixes of Phase 12. The typical time dependence observed with mixes containing lower levels of aluminate show a slow increase over time before leveling off at a final value. In contrast, the mixes of Phase 12 show a peak in E after which the value decreases. An explanation for these results is the formation of microcracks within the cylinder that disrupt strength properties of the cured monolith. This is further validated by the fact that the response of the measurement (resonant frequency) becomes very broad. Typically, the signal is quite narrow reflective of a homogenous sample.

All of these samples had been removed from the molds and measured a number of times which could have initiated or accelerated the cracking. Nevertheless, this reduction in E over time is suggestive of a negative consequence of increased levels of aluminate in the salt solution. If the cracking is caused by high aluminate content, it would lead to higher permeability of the Saltstone over relatively short time periods (100's of days). Further work will be required to confirm this explanation.

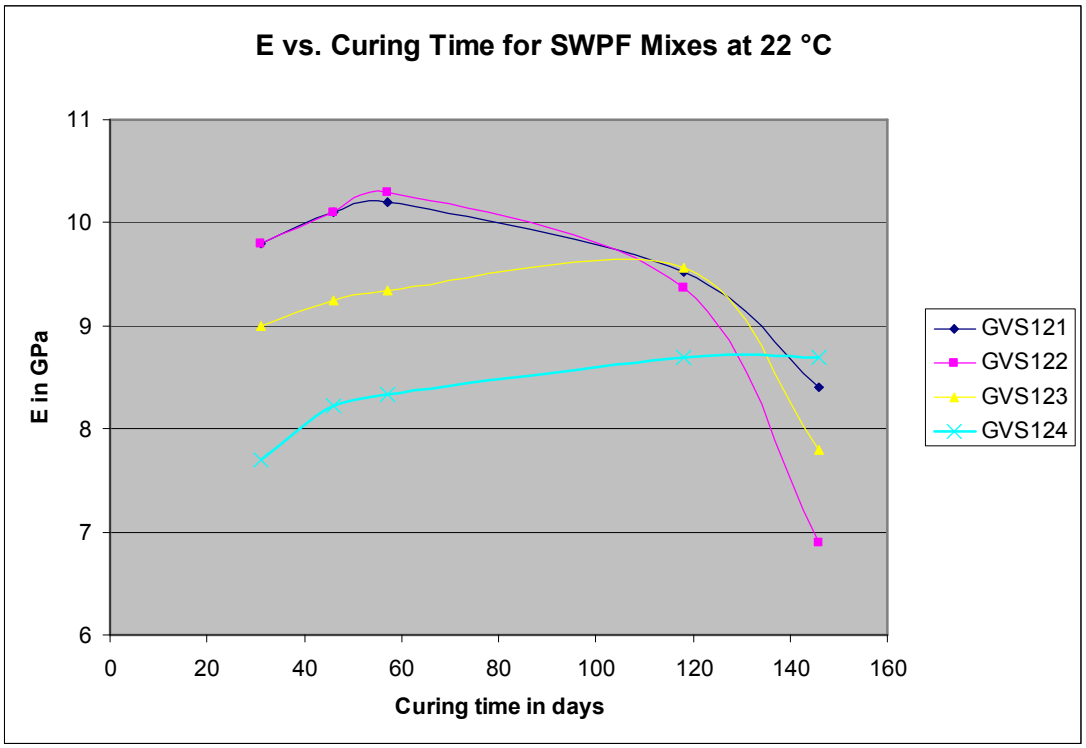

Figure 3-5 E vs. curing time at 22 °C for GVS121 through GVS124.

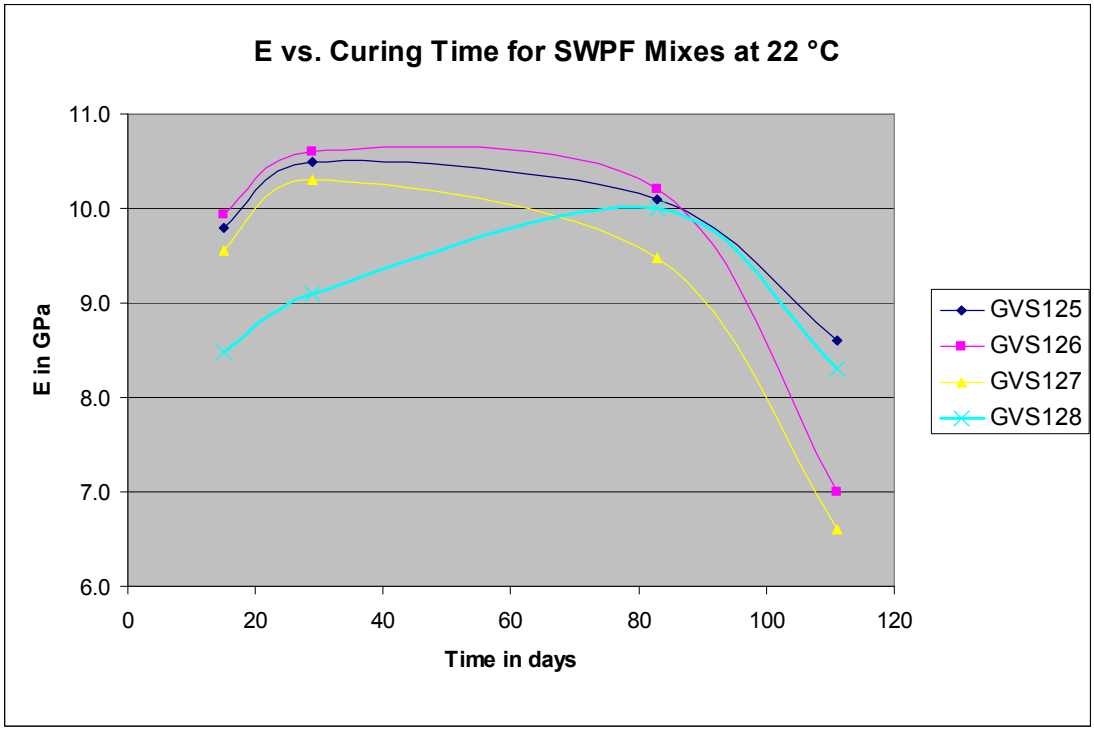

Figure 3-6 E vs. curing time at 22 °C for GVS125 through GVS128.

3.3 Young's Modulus as a Function of Curing Temperature

It has been shown previously that E, in general, decreases with increasing curing temperature. The results for Phase 12 of the Variability Study (Table 3-4) are consistent with these previous findings but reveal a dependence on aluminate concentration over the increased range of 0.35 to 0.65 M in the salt solution. As the aluminate concentration increases, the reduction in E at higher temperatures of curing is mitigated. Furthermore, the mixes with higher slag content show significantly less reduction in E at higher curing temperatures. These trends are shown graphically in Figures 3-7 and 3-8.

Table 3-4. Young's Modulus Values for Phase 12 Mixes as a Function of Curing Temperature.

Mix Number	E (GPa)	E (GPa)	E (GPa)
	Cured at 22 °C	Cured at 40 °C	Cured at 60 °C
GVS121	9.8	6.8	3.5
GVS122	9.8	7.2	3.8
GVS123	9.0	7.2	4.2
GVS124	7.7	7.1	4.7
GVS125	10.5	NM	7.0
GVS126	10.6	NM	7.7
GVS127	10.3	NM	7.9
GVS128	9.1	NM	8.2

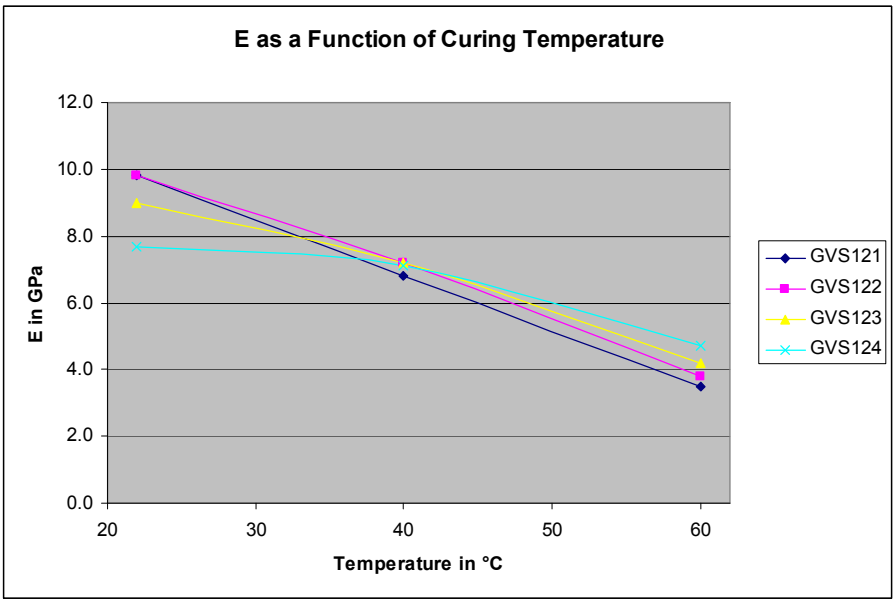

Figure 3-7. Young's modulus (E) values as a function of curing temperature for GVS121 through GVS124.

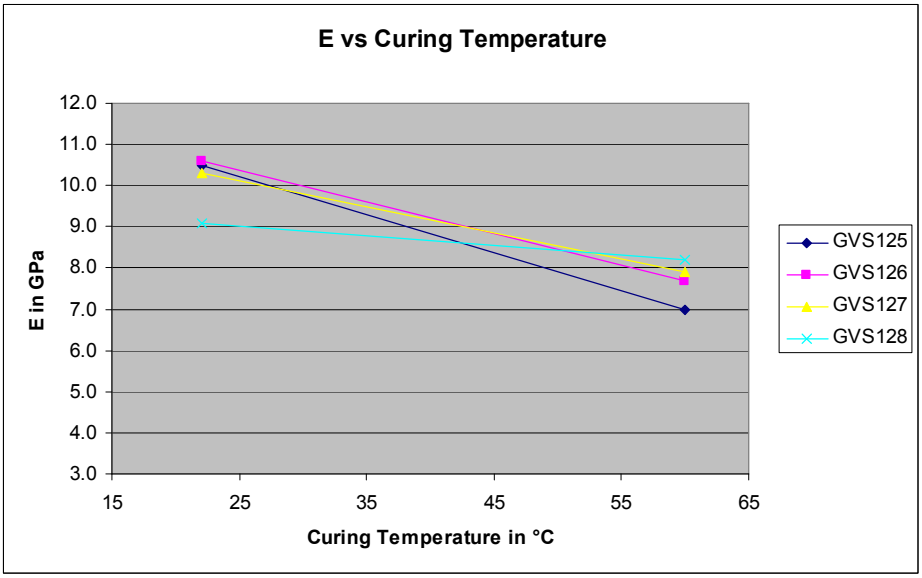

Figure. 3-8 Young's modulus (E) values as a function of curing temperature for GVS125 through GVS128.

The time dependence of E values at 40 °C and 60 °C are provided in Figures 3-9, 3-10 and 3-11. All of these plots show that the E values level off early and do not decrease over time. This is in contrast to the time dependent results for the samples cured at 22 °C in which E peaked and then began to decrease with time. This suggests that no cracking is occurring in the samples cured at higher temperatures over the time of measurement. For all three curing temperatures, the samples were sealed and handled equivalently such that the only difference was the temperature of curing.

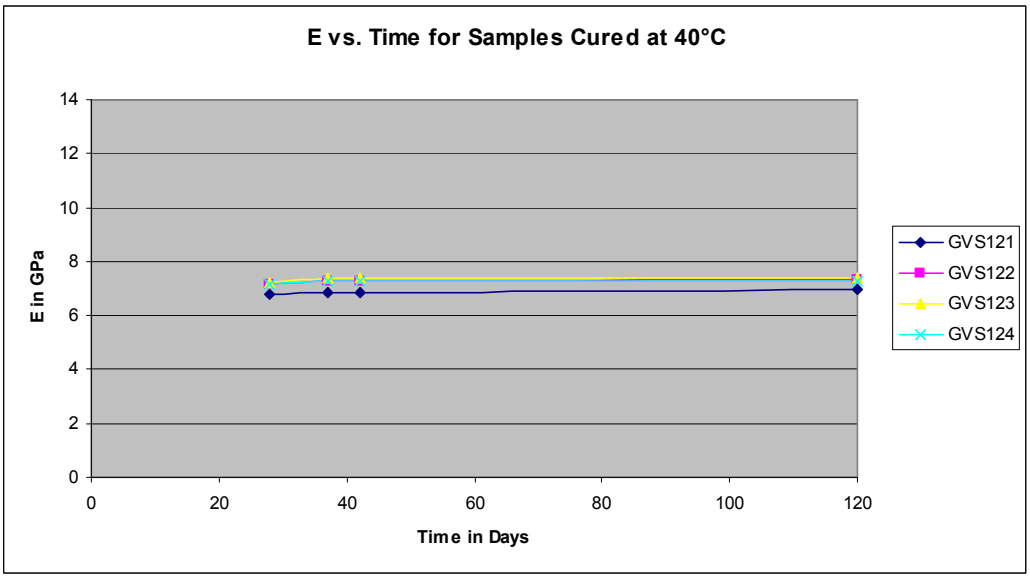

Figure 3-9. Time dependence of E for samples cured at 40 °C for 28 days.

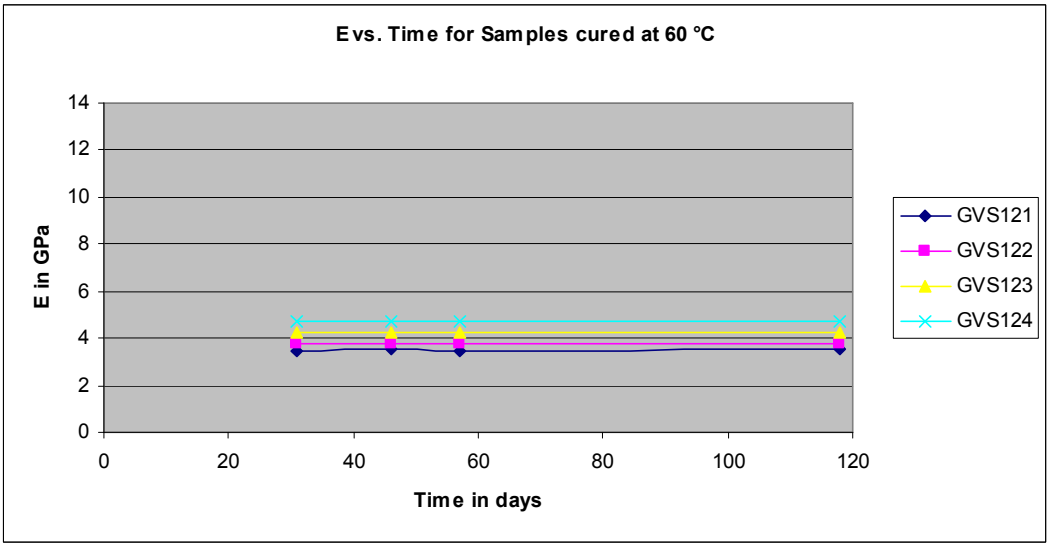

Figure 3-10. Time dependence of E for samples cured at 60 °C for 28 days.

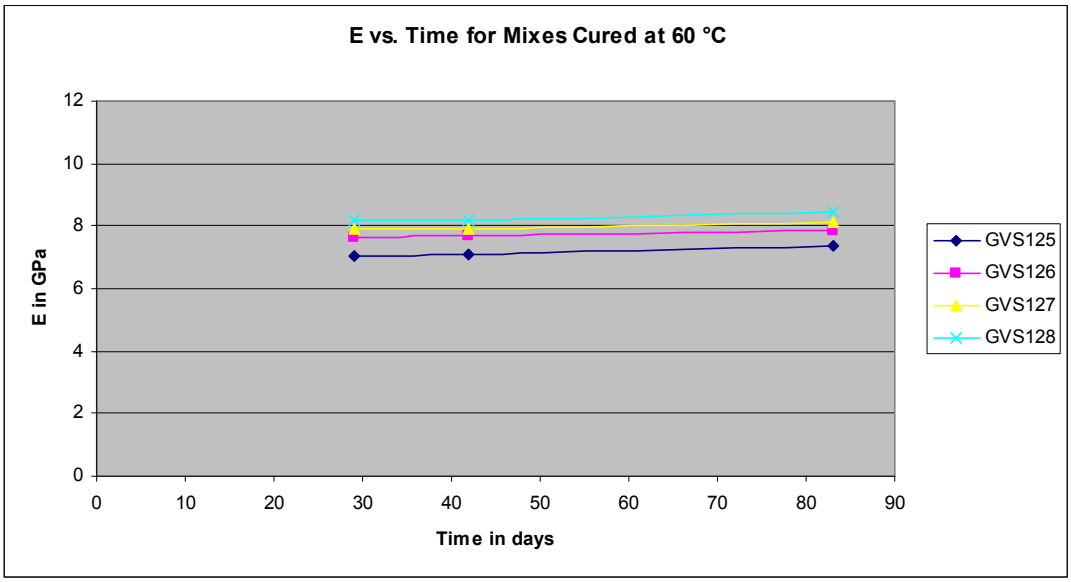

Figure 3-11. Time dependence of E for samples cured at 60 °C for 28 days.

3.4 Reproducibility of Young's Modulus

Batch-to-batch reproducibility was determined for Young's modulus and the cured grout density for three of the mixes, GVS121 through GVS123 (Table 3-5). The mixes were batched approximately 10 days apart with the later batch represented by the suffix R in the batch number.

Table 3-5. Measurement of Reproducibility for GVS121-123.

	Young's Modulus			Cured Density		
	22 °C	40 °C	60 °C	22 °C	40 °C	60 °C
GVS121	9.77	6.96	3.64	1.76	1.77	1.76
GVS121R	9.81	6.80	3.48	1.76	1.77	1.77
% difference	-0.4%	2.3%	4.4%	-0.2%	0.2%	-0.6%
GVS122	9.73	7.31	3.87	1.75	1.76	1.76
GVS122R	9.82	7.20	3.76	1.75	1.75	1.76
% difference	-0.9%	1.5%	2.8%	-0.1%	0.6%	0.1%
GVS123	8.78		4.19	1.77		1.77
GVS123R	8.96		4.23	1.75		1.76
% difference	-2.1%		-1.0%	1.1%		0.6%

The batch-to-batch reproducibility of Young's modulus is excellent for these mixes at three different curing temperatures. This reproducibility is important to the anticipated use of E as an indicator and differentiator of performance for Saltstone mixes. The greatest percentage error (4.4%) occurred with the lowest value of E for GVS121 at a curing temperature of 60 °C.

The cured grout densities were obtained by calculating the volume of the cylinder from the measured dimensions and dividing by the total mass of the cylinder. These results are also very

reproducible. It is interesting to note that the measured densities of these mixes at all three curing temperatures were consistent over this curing temperature range.

3.5 Young's Modulus at Different Time/Temperature Curing Profiles

Previous results [4] have shown that the performance properties of the mixes depend on the time/temperature profile for curing. Figure 3-12 shows the dependence of E on time and temperature curing profiles for a mix at 0.60 w/cm ratio, 45 wt% slag and 0.55 M aluminate (GVS123). The time/temperature curing profile for each curve is provided in the chart below the figure. The data show that an increase in temperature to 60 °C after 1 to 3 days curing at 22 °C results in E values that are less than the mix cured only at 22 °C. The GVS123K-2 mix that has cured for only one day at 22 °C prior to curing at 60 °C does not reach as high an E value as the GVS123K-3 mix which cured initially at 22 °C for 3 days. The dip in the curve for the GVS123K-2 mix correlates with the appearance of surface cracking on this cylinder. For any of the mixes cured initially at 60 °C or 75 °C, the measured E values are all low and do not improve even after additional curing at 22 °C. The final mix, GVS123K-9, which was cured for 1 day at 22 °C followed by 6 days at 75 °C, showed considerable surface cracking (see Figure 3-22). Figure 3-12 also shows the results for curing temperature profiles at 40 °C and 75 °C. The samples cured at 75 °C had the lowest values of E. Those samples cured at 40 °C had E values between the values for samples cured at 22 °C and the values for samples cured at 75 °C.

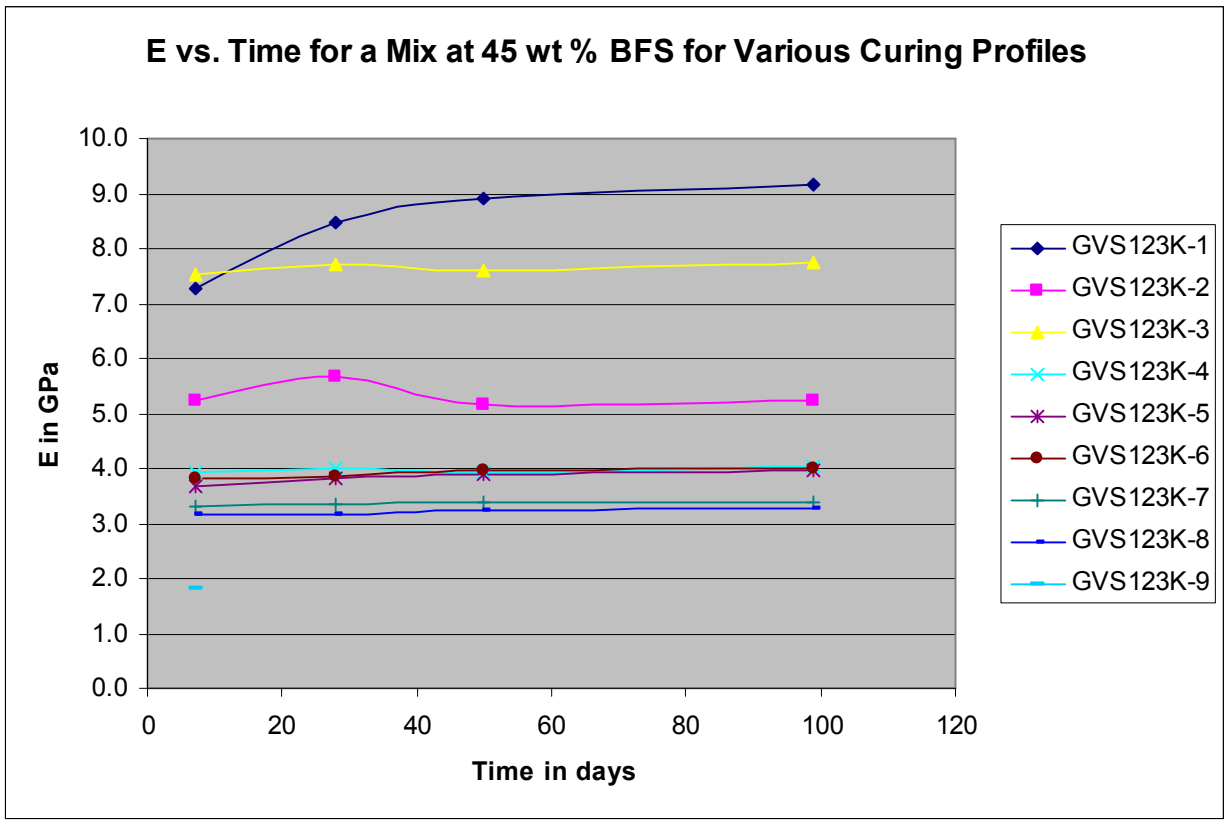

TR #	Time/ Temperature Profile	TR #	Time/ Temperature Profile
GVS123K-1	Curing only at 22 °C	GVS123K-6	3 days at 60 °C and 4 days at 22 °C
GVS123K-2	1 day at 22 °C and 6 days at 60 °C	GVS123K-7	7 days at 75 °C
GVS123K-3	3 days at 22 °C and 4 days at 60 °C	GVS123K-8	1 day at 75 °C and 6 days at 22 °C
GVS123K-4	7 days at 60 °C	GVS123K-9	1 day at 22 °C and 6 days at 75 °C
GVS123K-5	1 day at 60 °C and 6 days at 22 °C		

Figure 3-12. Time dependence of E (GPa) for GVS123 (45 wt % slag) at indicated time and temperature profiles.

In general, similar trends in E were obtained for the mixes containing 60 wt % BFS (GVS127) under similar conditions of time and temperature (see Figure 3-13). However, these values of E are higher than the mixes containing 45 wt % BFS, suggesting higher levels of slag are beneficial in terms of performance over this range of time and temperature curing profiles.

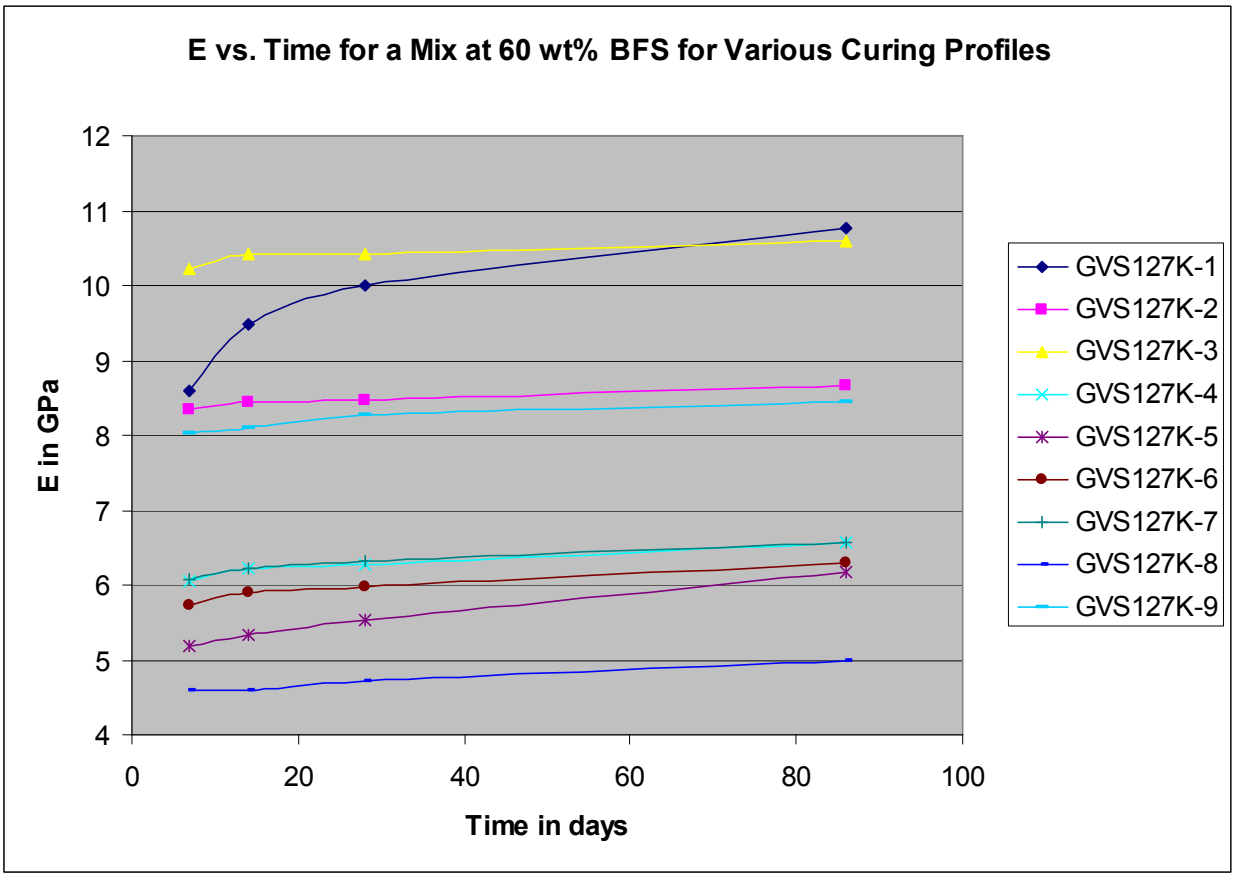

TR #	Time/ Temperature Profile	TR #	Time/ Temperature Profile
GVS127K-1	Curing only at 22 °C	GVS127K-6	3 days at 60 °C and 4 days at 22 °C
GVS127K-2	1 day at 22 °C and 6 days at 60 °C	GVS127K-7	7 days at 75 °C
GVS127K-3	3 days at 22 °C and 4 days at 60 °C	GVS127K-8	1 day at 75 °C and 6 days at 22 °C
GVS127K-4	7 days at 60 °C	GVS127K-9	1 day at 22 °C and 6 days at 75 °C
GVS127K-5	1 day at 60 °C and 6 days at 22 °C		

Figure 3-13. Time dependence of E (GPa) for GVS127 (60 wt % slag) at indicated time and temperature profiles.

3.6 Porosities as a Function of Curing Temperature

The impact of aluminate molarity in the salt solution and slag content in the premix on total porosity, Φ, was determined for the Phase 12 SWPF mixes. The total porosity values (expressed as fractions) for samples cured at three different temperatures are shown in Table 3-6. The total porosity decreased with increasing curing temperature for all mixes except GVS128. The mixes at 45 wt % slag had higher porosities than the corresponding samples batched with 60 wt % slag and the results are consistent with E values. Also, the trend observed for Φ as aluminate concentrations increased is generally consistent with E values over this range.

Table 3-6. Total Porosity (Φ) for Mixes Batched with either 45 or 60 wt% Slag as a Function of Aluminate Molarity.

Total Porosity			
	22 °C	40 °C	60 °C
	32 days	37 days	32 days
GVS121	0.570	0.584	0.607
GVS122	0.576	0.576	0.606
GVS123	0.572	0.589	0.611
GVS124	0.573	0.584	0.604
	29 days	29 days	29 days
GVS125	0.533	0.562	0.584
GVS126	0.541	0.557	0.573
GVS127	0.542	0.559	0.562
GVS128	0.552	0.559	0.554

3.7 Heat of Hydration at Elevated Temperature

As previously discussed, the heat of hydration data can be used to estimate the degree of hydration of cementitious materials. From the data presented thus far, higher curing temperatures generally decrease the values of the performance properties. This reduction in performance at higher curing temperatures could be due to a lower degree of hydration at the higher temperature and to changes in the microstructure of the grout with curing temperature. In an effort to determine whether a reduction in degree of hydration occurs at higher curing temperatures, measurements of the heat of hydration were made at a higher temperature. These initial experiments were limited (due to FY09 budget constraints) to an elevated isothermal temperature of 50 °C for a set of 8 mixes.

Two reference mixes were batched and monitored using isothermal calorimetry to provide a comparison of the heats of hydration for simpler systems at 25 °C and 50 °C. The first reference mix (reference mix 1) was portland cement in water at a w/c ratio of 0.60. Previous calorimetric testing of this mix containing Type II portland cement obtained from SPF revealed that ~ 400 J/g of cement were released at an isothermal temperature of 25 °C over 28 days. The top curve of Figure 3-14 shows the heat generation for this mix over 16 days at 25 °C while the bottom curve of Figure 3-14 shows the heat of hydration data for 16 days at 50 °C. Comparison of the two curves reveals that the initial rate of hydration is faster at 50 °C. This is consistent with literature results that show in general, higher curing temperatures increase the rates of hydration [11]. The hydration reactions at 50 °C leveled off by 16 days in contrast to those at 25 °C where the heat generation was still increasing at 16 days. The total heat of hydration was roughly the same for the two temperatures with values of 400 J/g at 25 °C (at 28 days) and 390 J/g at 50 °C. The reduction in heat production at 50 °C is 2.5%. The results demonstrate that curing the cement in water mix at 50 °C accelerates the hydration reactions but generates roughly an equivalent amount of heat, and has the same degree of hydration, as the mix cured at 25 °C.

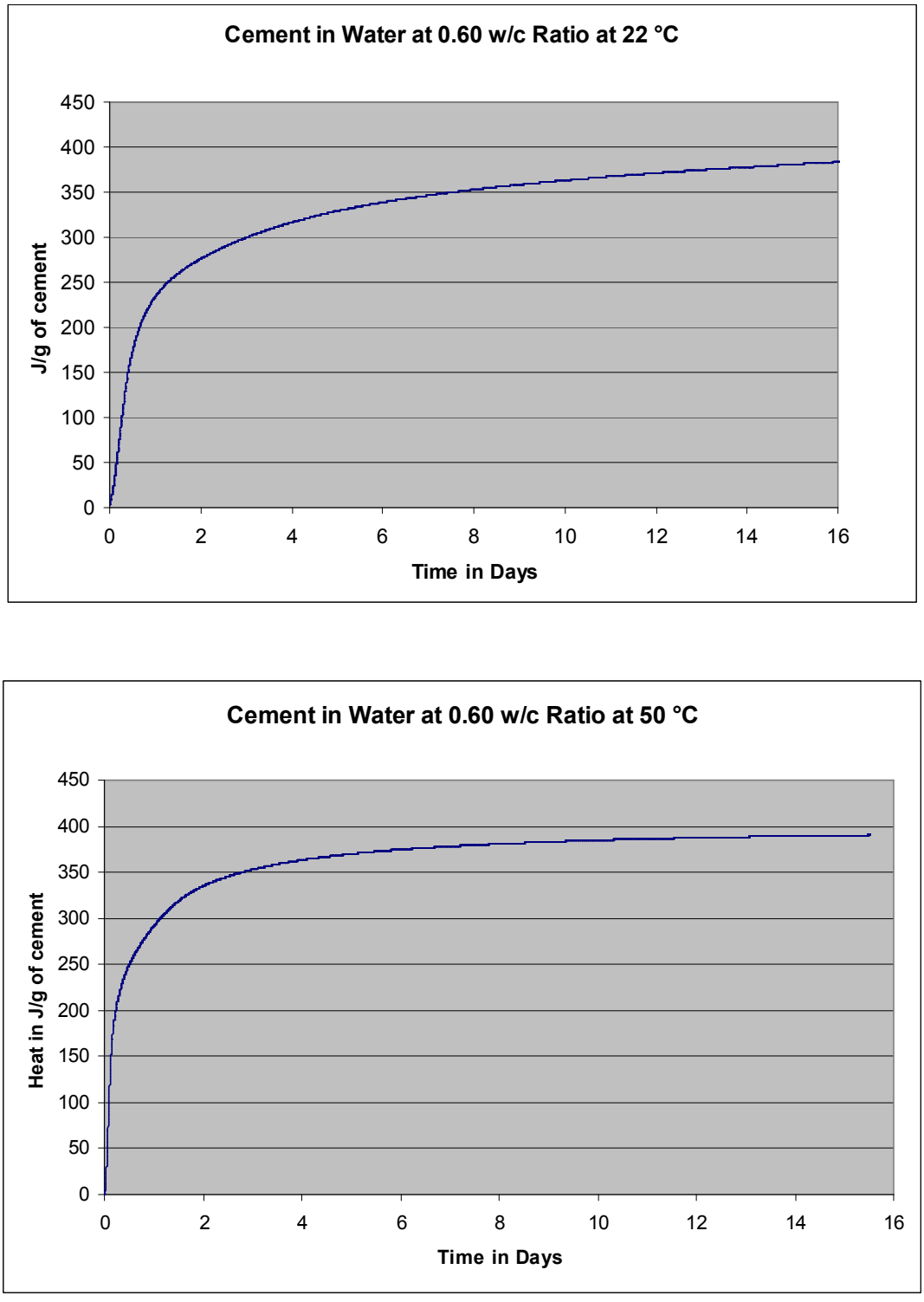

Figure 3-14 Comparison of heat of hydration at 25 °C (top curve) and 50 °C (bottom curve) for reference mix 1 of portland cement in water at 0.60 w/c ratio.

The second reference mix (reference mix 2) was a mix of 4.0 M NaOH solution and blast furnace slag at a 0.60 water to slag ratio. The heat of hydration for this mix at 50 °C is shown in Figure

3-15. For comparison, the heats of hydration curves for slag in water as a function of NaOH concentration at 25 °C are shown in Figure 3-16. The top curve in Figure 3-16 is the total heat released from a slag mix with 4.0 M NaOH at a 0.60 water to slag ratio at 25 °C. As was the case for the reference mix 1, the rate of hydration for reference mix 2 is higher at 50 °C compared to the mix at 25 °C. For example, it takes 5 days at 50 °C to reach a total heat output of 300 J/g compared to 10 days to reach the same value at 25 °C. The slag hydration reaction continues at both 25 °C and 50 °C over the experimental time frame, indicating the slag hydration reaction has a slower rate than portland cement hydration reaction under these conditions. The normalized maximum heat generation for slag at 25 °C is ~ 400 J/g while the maximum at 50 °C is ~ 390 J/g which corresponds to a 2.5% reduction in heat production at 50 °C relative to 25 °C. Therefore, the degree of hydration of slag in 4.0 M NaOH is also reduced by 2.5% at 50 °C.

In summary, both reference mixes showed similar responses. That is, the rate of hydration at 50 °C is greater than at 25 °C and the total amounts of heat (and consequently the degrees of hydration) are roughly the same at both temperatures. These responses are typical of cement in water mixes reported in the literature and therefore confirm the validity of the experimental measurements of heats of hydration at these higher temperatures [11].

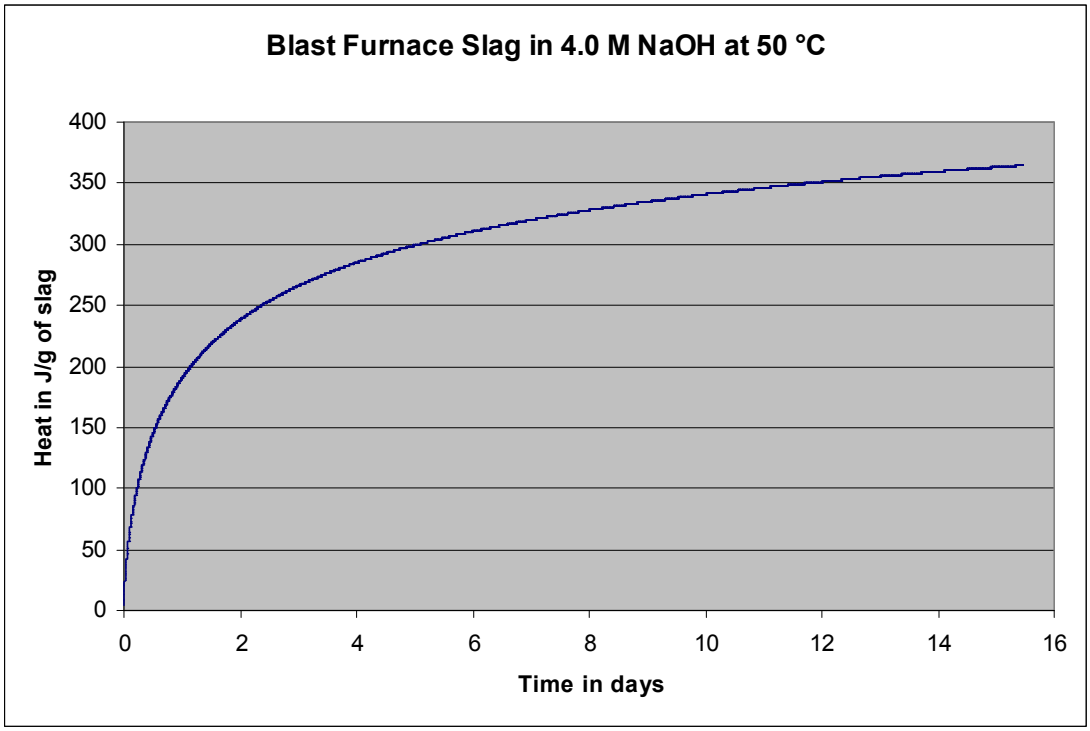

Figure 3-15. Heat of hydration measured at 50 °C for reference # 2, a mix containing blast furnace slag in a 4.0 M NaOH solution at a water to slag ratio of 0.60.

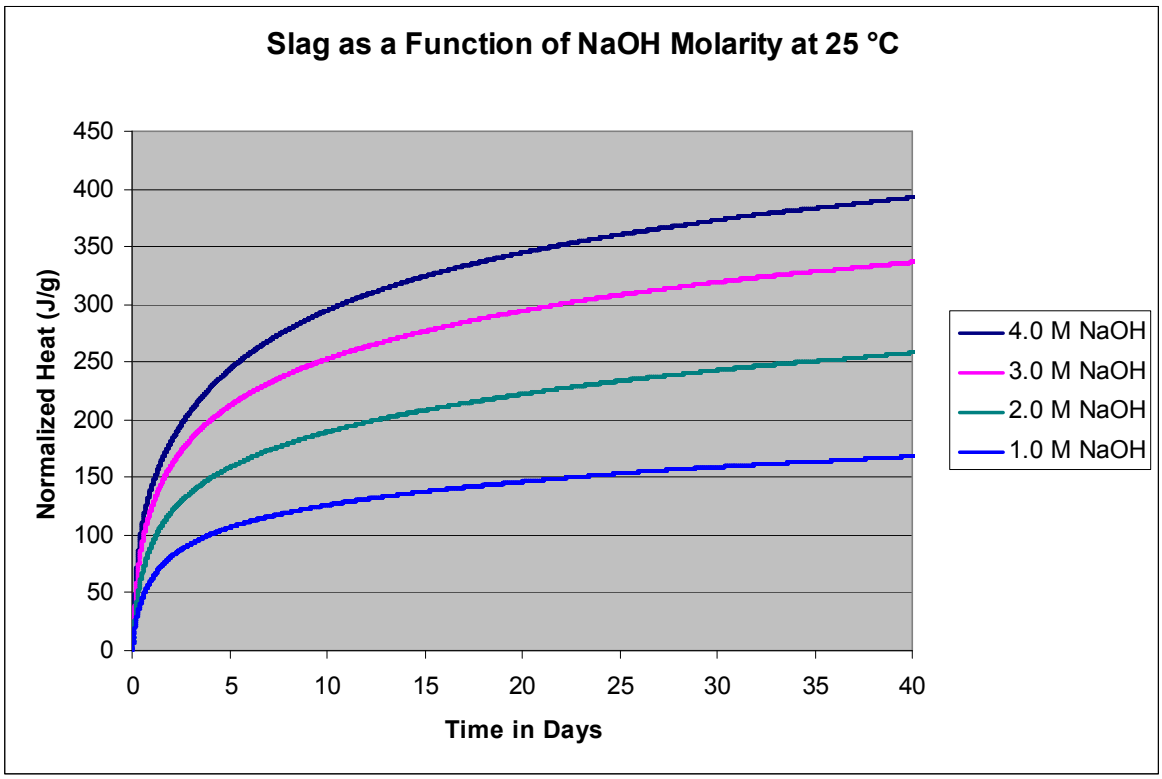

Figure 3-16. Heats of hydration of blast furnace slag in NaOH at 25 °C at a water to slag ration of 0.60. The top curve is for slag in a 4.0 M NaOH (reference # 2).

The heats of hydration at 25 °C and 50 °C for an SWPF mix containing 0.28 M aluminate at 0.55 w/cm and 52.5 wt % slag (center point for Phase 8 of the Variability Study) were measured and the results are presented in Figure 3-17. Consistent with the responses of both of the reference mixes, measurement at an isothermal temperature of 50 °C accelerated the hydration reactions of the SWPF mix relative to curing at 25 °C. In addition the induction period typically observed at 25 °C for high aluminate mixes, was significantly reduced at 50 °C. However, in contrast to the two reference mixes, measurement of the SWPF mix at 25 °C resulted in a total heat output of 230 J/g of cementitious materials compared to measurement at 50 °C which resulted in a total heat output of 185 J/g of cementitious materials. Therefore, the higher isothermal temperature reduced the heat of hydration, and consequently the degree of hydration, of the SWPF mix by 20%. This suggests that at least some of the reduction in performance properties may be due to a reduction in the degree of hydration at higher curing temperatures. Although the isothermal calorimetry was performed at 50 °C, most of the performance measurements were made on samples cured at 40 °C and 60 °C. Therefore, it is possible that measurement at 60 °C may result in a further reduction in degree of hydration. Additional testing will be required to confirm this.

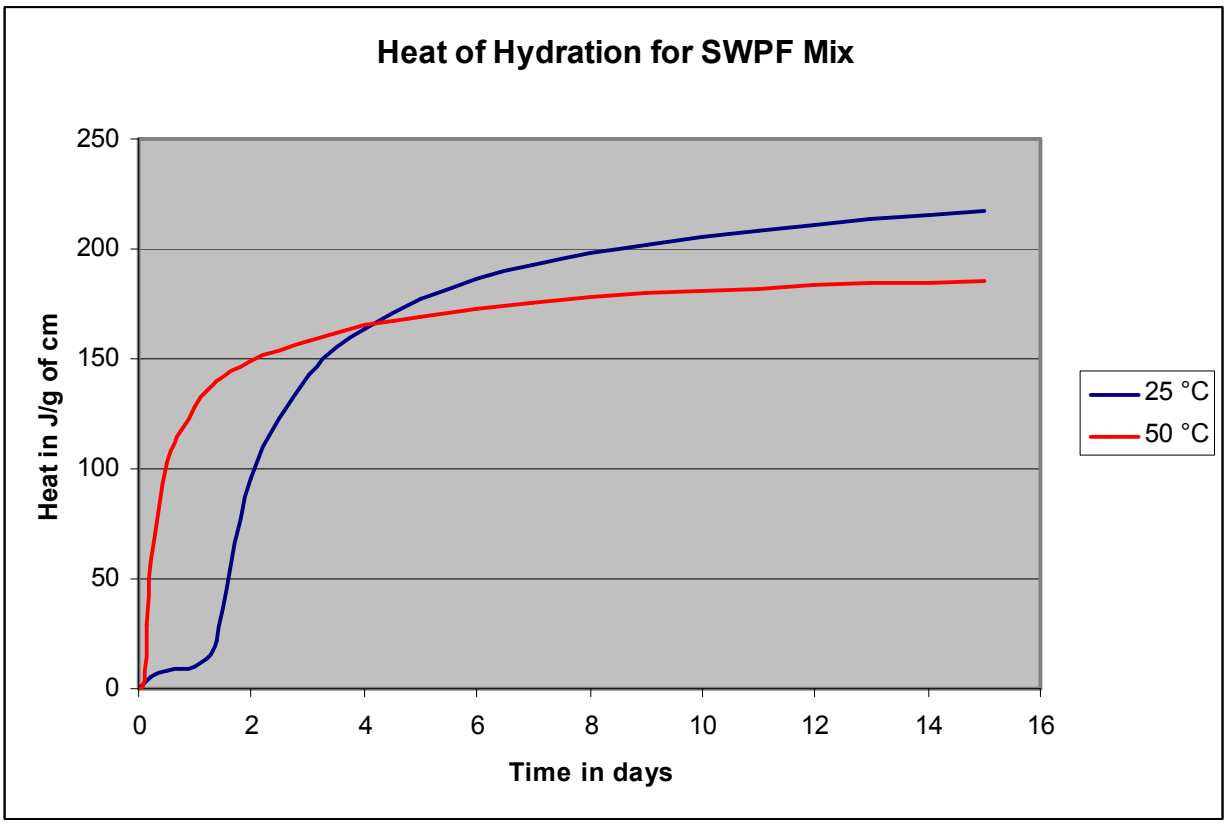

Figure 3-17. Comparison of the heats of hydration of an SWPF mix with 0.28 M aluminate at 25 °C and 50 °C.

The SWPF calorimetric data presented in Figure 3-17 are for a mix containing 0.28 M aluminate. An SWPF mix containing the originally projected aluminate level of 0.114 M was also tested. Figure 3-18 provides the 50 °C heat of hydration data for an SWPF mix at 0.60 w/cm ratio at the normal 45:45:10 premix distribution and an aluminate concentration of 0.114 M. The heat of hydration is ~180 J/g of cementitious materials for this mix measured at 50 °C which is essentially equivalent to what has been observed at a measurement temperature of 25 °C. Therefore, the results with this mix at the two measurement temperatures are consistent with the results of the two reference mixes but different from the results of the SWPF mix containing 0.28 M aluminate. That is, at low aluminate levels, the degree of hydration for the SWPF mix at 0.114 M aluminate is roughly the same at both 25 °C and 50 °C in contrast to the SWPF mix with 0.28 M aluminate where a 20% reduction in the heat of hydration was observed at 50 °C relative to 25 °C. However, in both cases the rate of hydration increased at 50 °C. Also, the rate of the hydration for the lower aluminate SWPF mix was slower over the initial few days than the rate for the SWPF mix with higher aluminate.

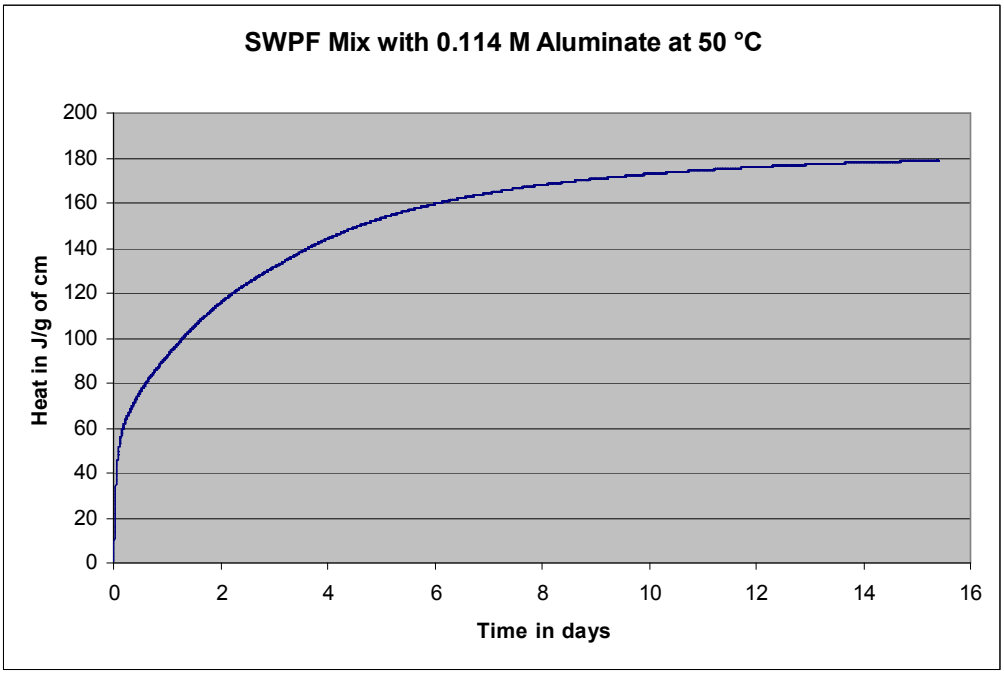

Figure 3-18. Heat of hydration at 50 °C for an SWPF mix with 0.114 M aluminate.

The measurements of heats of hydration at 50 °C were also performed using ARP/MCU mixes [10]. The heat of hydration results obtained for ARP/MCU mixes batched with 0.05 M (GVS107) and 0.22 M aluminate (GVS110) at different measurement temperatures were consistent with the responses observed for the SWPF mixes at two levels of aluminate. The heats of hydration at 25 °C for the ARP/MCU mixes are shown in Figure 3-19 and reveal that the higher aluminate mix generated 203 J/g as compared to only 140 J/g for the low aluminate mix.

The heats of hydration results at 50 °C (Figure 3-20) show that the 0.05 M aluminate mix produces roughly the same amount of heat (and consequently, the same degree of hydration) but at a somewhat faster rate than at 25 °C. On the other hand, the mix at 0.22 M aluminate produced only 162 J/g at 50 °C in contrast to the 203 J/g released at 25 °C (Figure 3-21). This is a reduction in the heat production of 20%. As was the case for the high aluminate SWPF mix, the ARP/MCU mix with a higher level of aluminate also had a lower degree of hydration at 50 °C. The induction period for GVS110 was reduced at 50 °C relative to 25 °C and in both cases measurement at 50 °C resulted in higher rates of hydration.

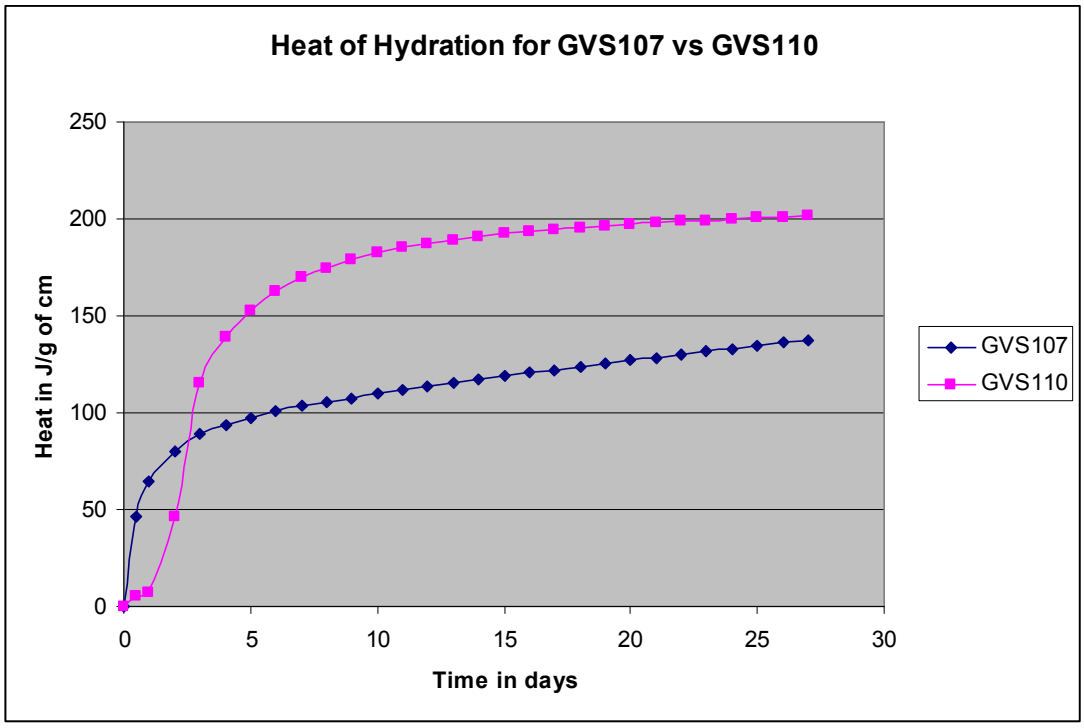

Figure 3-19. Comparison of heats of hydration for GVS107 (0.05 M aluminate) and GVS110 (0.22 M aluminate) at 25 °C.

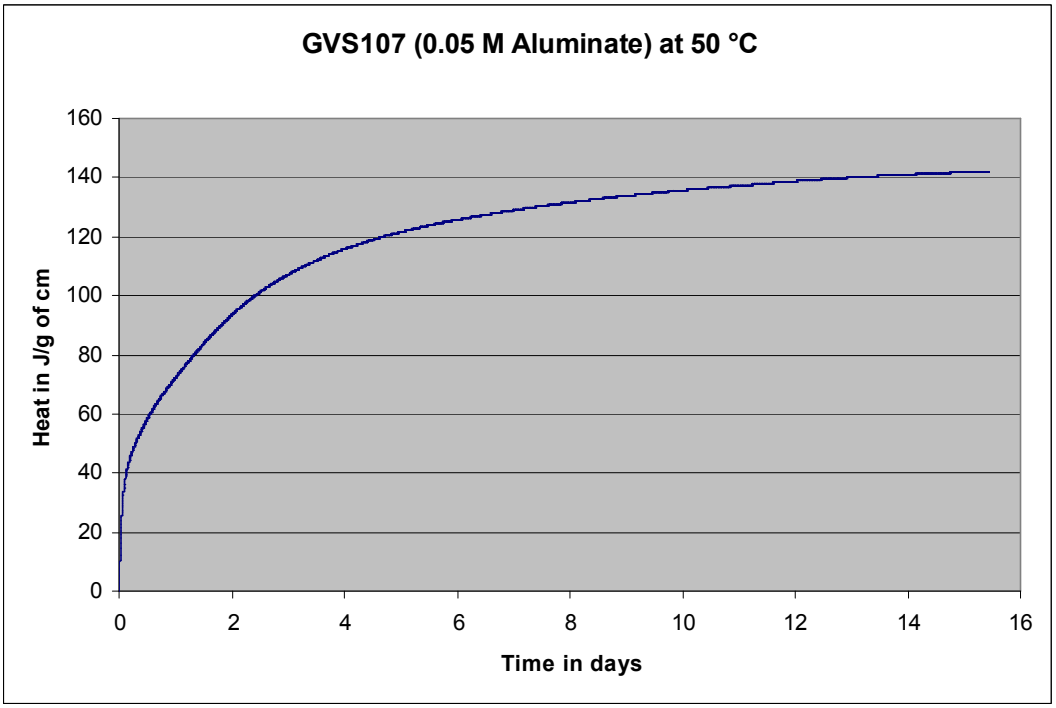

Figure 3-20. Heat of hydration for GVS107 at 50 °C.

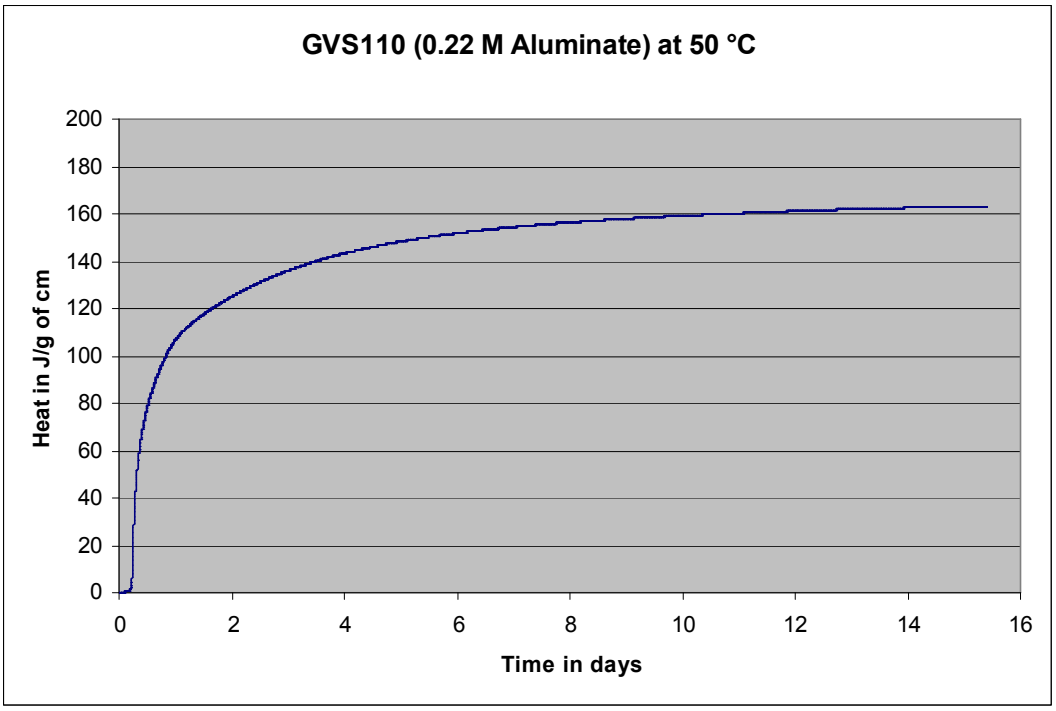

Figure 3-21. Heat of hydration for GVS110 at 50 °C.

These results show the dependence of the heat of hydration on the concentration of aluminate in the salt solutions of the SWPF and the ARP/MCU simulants. For low concentrations of aluminate, the heats of hydration are roughly the same at both 25 °C and 50 °C. In contrast, higher concentrations of aluminate in the salt solutions lead to a 20% reduction in the heats of hydration at 50 °C. The lower heat of hydration reflects a lower degree of hydration which in turn leads to decreased performance of the Saltstone mixes.

On the other hand, mixes with low concentrations of aluminate also show a reduction in performance properties at higher curing temperatures. Since the degree of hydration is roughly the same at the two temperatures, the differences in performance observed with the mixes are most likely due to microstructural changes between the two curing temperatures.

Previous results at 25 °C show that the degree of hydration of Saltstone mixes containing aluminate concentrations roughly less than 0.2 M, do not reach the expected values if the premix components hydrate independently [9, 10]. These previous results also show at 25 °C that the expected value of hydration is realized for aluminate concentrations greater than roughly 0.2 M. Therefore, aluminate at high enough levels in the salt solution can facilitate hydration and improve performance. The results of the higher temperature calorimetry suggest that increased temperatures can counteract this and reduce the degree of hydration to the levels seen at lower aluminate concentrations.

3.8 Processing Properties

Task 4 focused mainly on the performance properties of the SWPF Saltstone mixes. However, the processing properties must also be acceptable for processing at SPF. The processing property results for Phase 12 mixes are presented in Table 3-7. All of the mixes had gel times of 20 minutes or greater and were therefore acceptable. However, all of the mixes with 60 wt % slag had the shortest gel time of 20 minutes. The yield stress and plastic viscosity values were relatively low for all of the mixes. In fact the yield stress decreased as the level of aluminate increased. Acceptance criteria for the flow properties have yet to be established and pumping calculations will be required to determine these criteria. At 22 °C there was a small amount of bleed liquid on all of the mixes after both 1 and 3 days. Set times at 22 °C decreased as the aluminate concentration increased. Set times of 1 day were observed for samples cured at 40 °C and at 60 °C.

Table 3-7. Processing Properties for Phase 12 Mixes.

		Fresh	Cured		Uncorrected	1-Day Bleed				3-Day Bleed	Set Time		
Identifier	Gel Time	Density	Density	Flow	Yield Stress	Viscosity	22 °C	40 °C	60 °C	22 °C	22 °C	40 °C	60 °C
	minutes	g/mL	g/mL	cm	Pa	cP	Vol %	Vol %	Vol %	Vol %	Days	Days	Days
GVS121	30	1.727	1.763	24.2	2.5	67.1	<0.5	<0.2	0.0	<0.2	3	1	1
GVS122	30	1.730	1.753	25.0	2.3	68.2	<0.2	<0.2	0.0	<0.2	3	1	1
GVS123	40	1.726	1.771	25.0	2.0	67.7	<0.2	<0.2	0.0	<0.2	1	1	1
GVS124	40	1.731	1.763	25.6	1.9	69.6	<0.2	<0.2	0.0	<0.2	1	1	1
GVS125	20	1.750	1.779	23.4	3.4	75.2	<0.1	0.0	0.0	<0.1	3	1	1
GVS126	20	1.751	1.788	24.7	3.1	73.1	<0.1	0.0	0.0	<0.1	3	1	1
GVS127	20	1.755	1.778	24.6	2.8	74.0	<0.1	0.0	0.0	<0.1	1	1	1
GVS128	20	1.751	1.771	24.7	2.8	75.1	<0.1	0.0	0.0	<0.1	1	1	1

3.9 Cracking

One of the samples (GVS123K-9) from the time temperature curing profile study with a 1 day cure at 22 °C followed by 6 days curing at 75 °C exhibited external cracking on the cast cylinder (Figure 3-22). This sample was sealed and did not dry out during this curing cycle. The Young's modulus value for this mix was 1.8 GPa, a very low value which most likely reflects cracking within the matrix. The cracks disrupt the overall strength of the cylinder and since E is correlated with compressive strength, its value also decreases. A hammer was used to strike the cylinder while contained inside a plastic bag. Pieces of the Saltstone were separated from the cylinder along the surface cracks. Visual examination of the pieces was consistent with a scenario where the cracks had extended into the cylinder prior to breakage (see Figure 3-23).

Figure 3-22. GVS123K-9 after 7 days.

Figure 3-23. GVS123K-9 after being struck by a hammer. The pieces that broke free followed the existing cracks.

3.10 Drying Shrinkage and Cracking

As part of task 4, a method was developed that can identify relative differences in the microstructure and permeability of grouts cured at different temperatures or as a result of variations in other key factors. The experiments performed were similar to those that were carried out with the ARP/MCU mixes [10] but in task 4, the cured, 2-inch diameter, cylindrical samples were dried in an oven at 60 °C to 65 °C for three days. The mass loss due to water evaporation after drying for each sample was measured and the samples were broken into two pieces by hand. This process revealed the cross-sectional areas of the cylinders after the drying and any changes in the microstructures as a function of curing temperature. Relative permeability can be discerned by the amount of water (measured mass loss) transferred through the porous medium and released to the atmosphere upon drying and the corresponding cross sectional images. Permeability and cracking will be discussed after results on the two reference cases are presented.

Two reference mixes were used during the development of this method. The first reference mix is an SWPF Saltstone sample with 0.14 M aluminate. Two samples from the same batch were cured at 22 °C and 60 °C for one week followed by curing for several months at ambient temperature. Both of these samples were then dried in the 60 °C oven for three days. Mass loss for the 22 °C cured sample is 19.8 wt % while the mass loss for the 60 °C cured sample is 23.8 wt %. The cross sectional area produced after breaking the sample cured at 22 °C is shown in Figure 3-24. The center core is still saturated with water and is dark blue-green in color. A diffuse outer core that is light blue-green in color is also evident and extends to within a centimeter of the surface. It is important to note that the photographs presented in this report were taken without a flash resulting in a false color. Therefore, the blue-green color is not evident in Figure 3-24. However, photographs for one set of samples both without and with a flash are provided for reference in Figures 3-28 and 3-29 and reveal the true colors.

Figure 3-24. Cross section of the cylinder initially cured at 22 °C and then heated in the oven at 65 °C for three days.

The cross sectional areas produced after breaking the samples cured at 22 °C and 60 °C are shown in Figure 3-25. The differences upon drying between the samples cured at 22 °C and at 60 °C are significant and reflective of different microstructures for the same starting material. The 60 °C cured cylinder broke into two pieces with smooth and flat fracture surfaces and there was no evidence of the water saturated core or blue-green color. The sample cured at 22 °C has a rough fracture surface which indicates cracking within the cylinder as a result of drying. The absence of a saturated core for the sample cured at 60 °C confirms the mass change data presented earlier and indicates the sample has a higher permeability than the sample cured at 22 °C.

Figure 3-25. Cross sectional views of samples cured at 22 °C (left) and 65 °C (right).

This method was developed in part as a result of recent results obtained on the hydraulic conductivity measured at MACTEC in Atlanta, Georgia for ARP/MCU samples [3]. This work was performed in a separate ongoing task as part of research to support the Performance Assessment of Saltstone. One of the 11 samples studied was cured at 60 °C for one week prior to subsequent curing at ambient temperature. Measurement of the permeability of this sample (in triplicate) was made at 25 °C. The hydraulic conductivity increased three orders of magnitude from ~ 10^{-9} cm/sec at 22 °C to ~ 10^{-6} cm/sec at 60 °C. Cross sectional images for the samples cured at 22 °C and 60 °C were similar to those observed for the SWPF reference case (Figure 3-25). The results therefore suggest that the microstructure observed in the SWPF sample cured at 60 °C is a highly porous solid grout with high permeability. Additional testing is required to confirm the effect of curing temperature on hydraulic conductivity since this conclusion is based on only one sample.

Cracking due to shrinkage in grouts and concretes is well known [11]. As Saltstone dries, an internal restraint is created by the process of differential drying. The grout shrinks as it dries but is internally restrained by the saturated core and when the tensile stress exceeds the tensile strength of the material, the grout cracks. Grouts and concretes have low tensile strengths which are typically on the order of 10% of the compressive strength value. The compressive strength of Saltstone mixes is generally low (~1000 psi) due to the high w/cm ratio to increase the waste loading and improve processing performance [9]. Therefore, the Saltstone mixes generally have low tensile strengths and can crack relatively easily upon drying.

The SWPF reference mix cured at 22 °C exhibited significant cracking after drying for 3 days. On the other hand, the reference mix cured at 60 °C showed no cracking upon drying even though more water was lost during drying at the higher temperature. In fact, the tensile strength

should be less for the sample cured at 60 °C based on lower values of Young's modulus for samples cured at higher temperatures. From this perspective, one would expect that the sample cured at 60 °C would have a higher degree of cracking. Further investigation into the microstructure of these mixes will be required to resolve this apparent discrepancy.

A second reference mix used in the development of this method was a grout produced from a 4.0 M NaOH solution mixed with blast furnace slag at a water to slag ratio of 0.60. The sample cured at 22 °C for one week lost 17.7 wt % while the sample cured at 60 °C lost 16.1 wt % after three days of drying at 65 °C. This mass loss as a function of curing temperature is opposite to the trend observed with the SWPF reference mix. Figure 3-26 shows the cross sections of samples cured at 22 °C and 60 °C. In both cases the dried grouts were highly fractured. The sample cured at 60 °C had a small core of saturated grout at the center (blue-green in true color) consistent with a slightly lower mass loss. Therefore, these results suggest that the sample cured at 60 °C had a roughly equivalent but lower permeability than the 22 °C cured sample. For this reference sample, the microstructure appears to be the same at both curing temperatures.

Figure 3-26. Cross sectional views of a mix batched from 4.0 M NaOH and slag cured at 22 °C (left) and 60 °C (right).

This method was next applied to the Saltstone mixes batched as part of Task 4 of the FY09 variability study. The mass losses for SWPF mixes, GVS121 – GVS124, as a function of curing temperature are provided in Figure 3-27. These mixes all contain the normal 45 wt % slag, 45 wt % fly ash and 10 wt % portland cement in the premix and the only variable is the concentration of aluminate in the SWPF simulant solution. The mixes (with the exception of GVS 121) lose less mass at 40 °C and more mass at 60 °C relative to the mixes cured at 22 °C. The SWPF mix, GVS121, was less sensitive to the curing temperature. The results for GVS121 samples are shown in Figure 3-28. For comparison, the same samples photographed with the flash (Figure 3-

29) reveal the blue green core and gray dried regions. For these samples, there is a decrease in the size of the saturated core with increasing curing temperature indicating the permeability increases with increasing curing temperature. The microstructure also changes as a function of curing temperature as evidenced by the reduction in cracking observed for the samples cured at 60 °C.

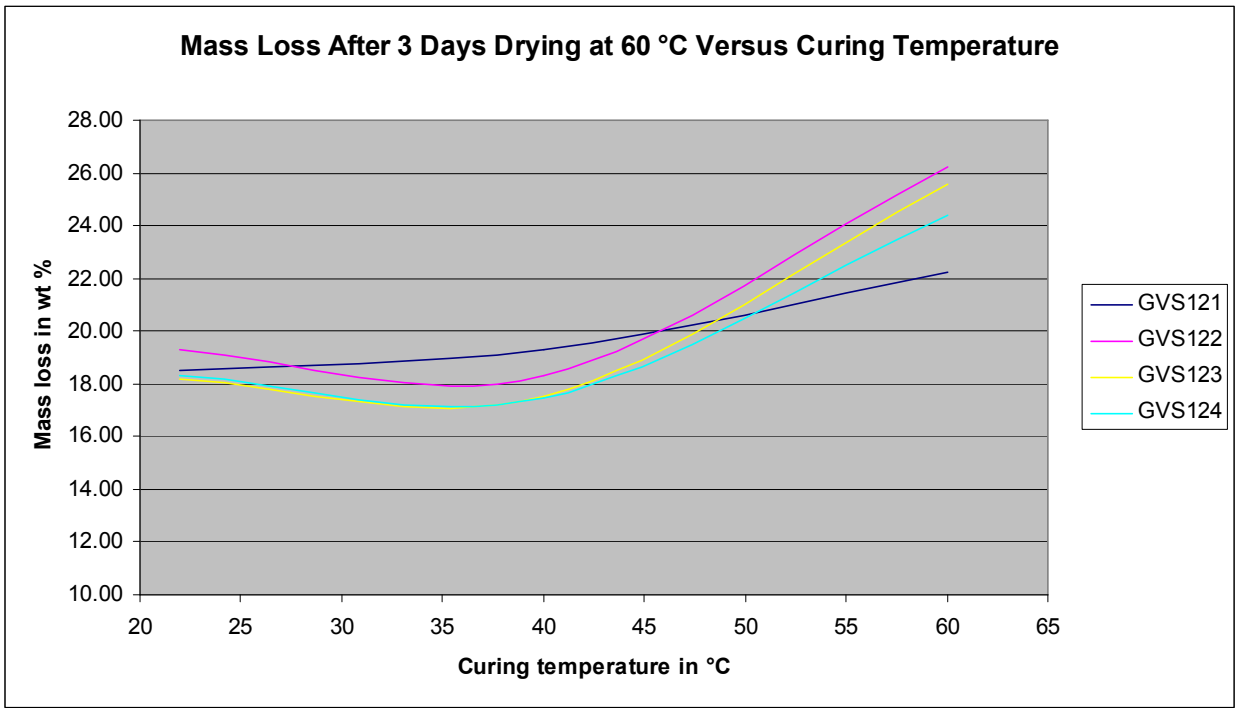

Figure 3-27. Mass change (wt %) for GVS121-GVS124 as a function of curing temperatures after 3 days at 60 °C.

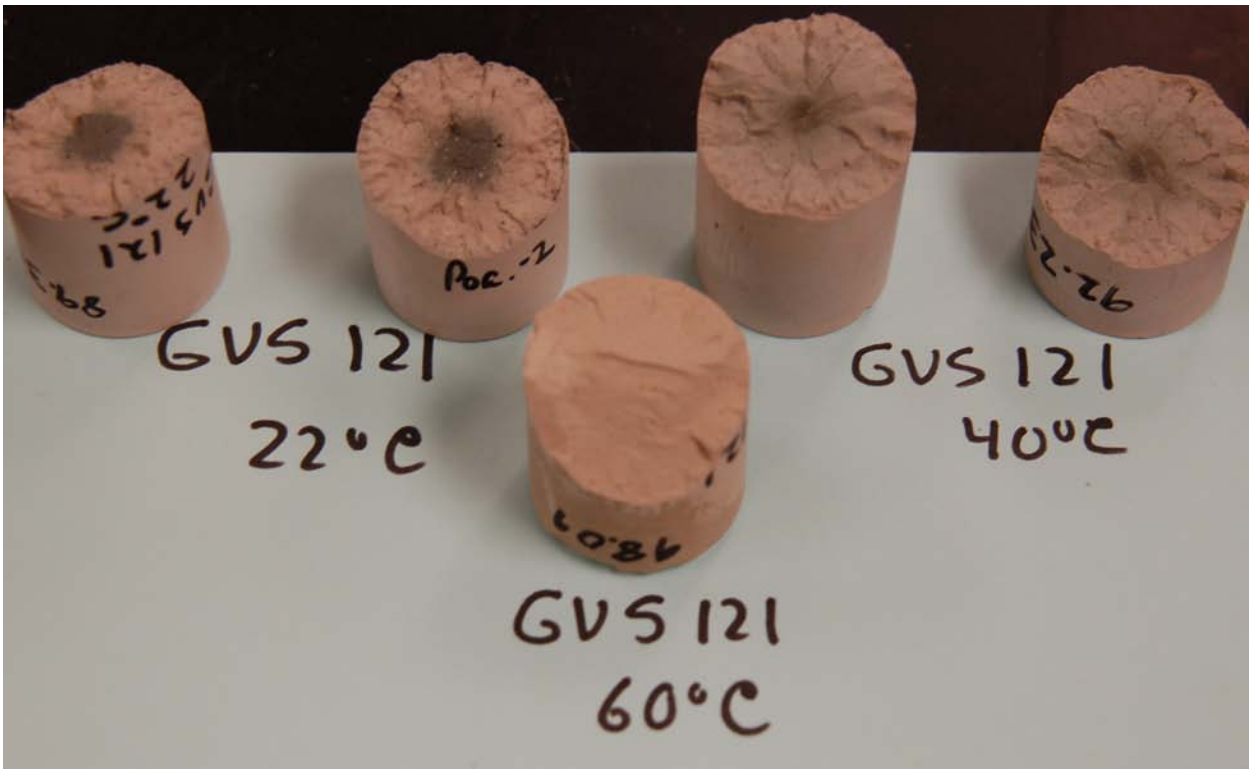

Figure 3-28 Photograph without a flash of GVS 121 samples cured at 22 °C, 40 °C and 60 °C.

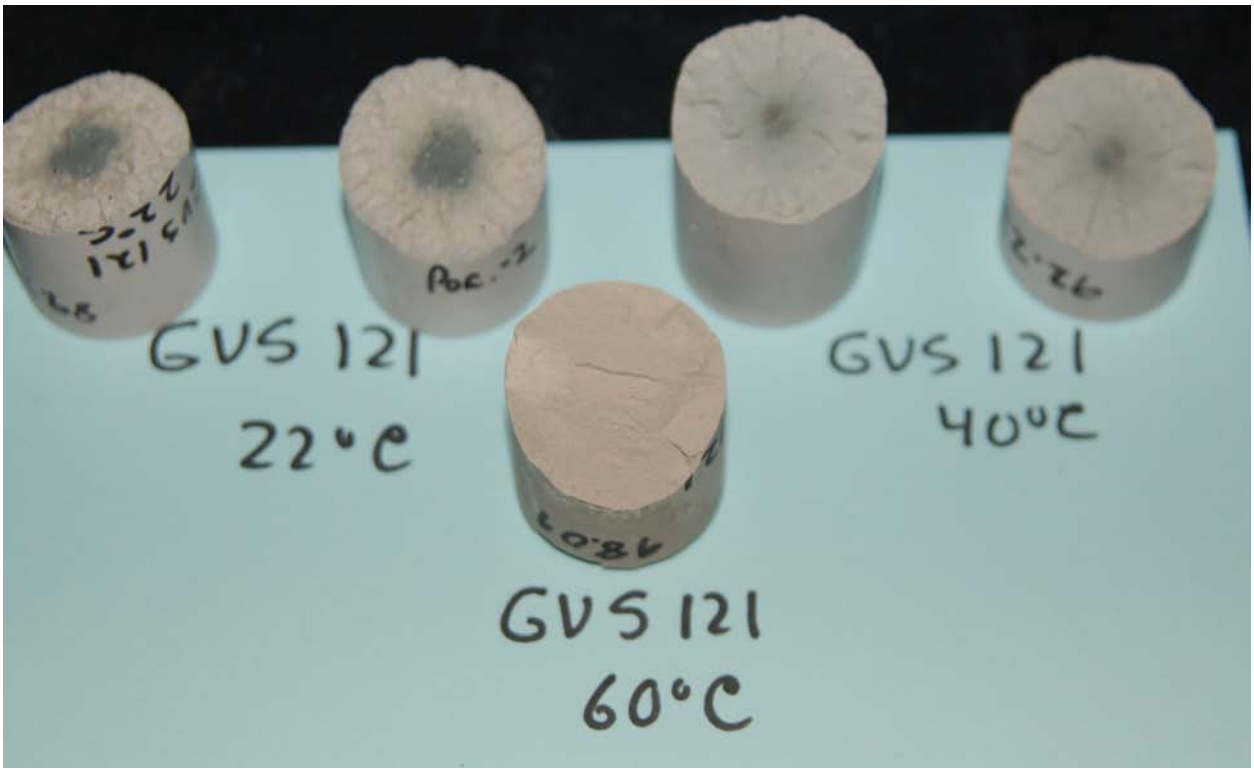

Figure 3-29. GVS 121 samples cured at 22 °C, 40 °C and 60 °C (with the flash and a blue background) showing a decrease in the size of the saturated core as the curing temperature is increased.

The GVS122 samples cured at 22 °C, 40 °C and 60 °C are shown in Figure 3-30. The saturated core is largest at 40 °C, consistent with the smallest mass change during sample curing. The same trend was also observed for mixes GVS123 and 124.

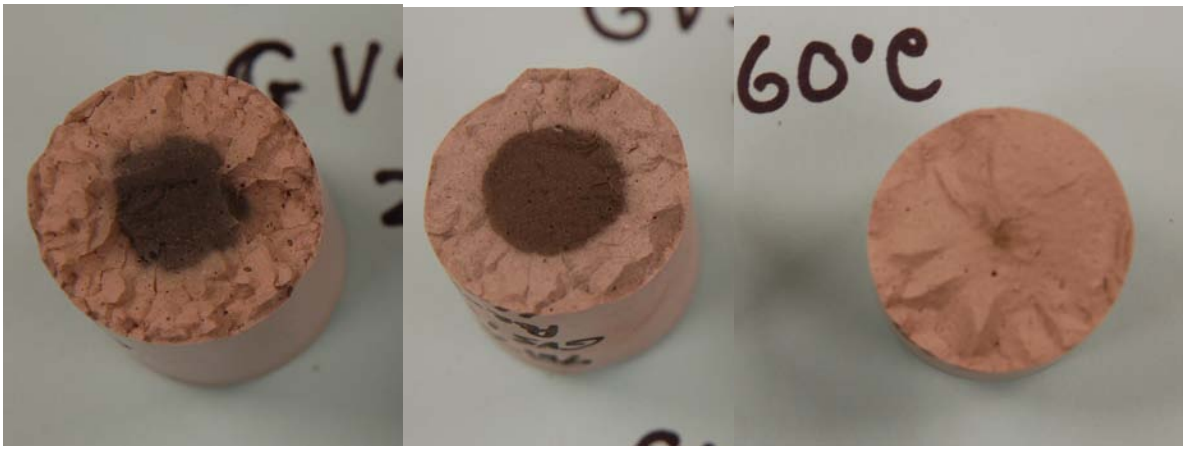

Figure 3-30. Samples of GVS122 cured at 22 °C (left), 40 °C (center) and 60 °C (right).

The results for GVS121 – GVS124 and for the reference SWPF sample with 0.14 M aluminate demonstrate that a curing temperature of 60 °C reduces the performance properties of the Saltstone mixes. Initial results suggest that permeability increases by 3 orders of magnitude for a sample cured at 60 °C vs. the same mix cured at 22 °C. The results are consistent with observed reduction in E for samples cured at 60 °C.

The mass losses for SWPF mixes, GVS125 – GVS128, as a function of curing temperature are provided in Figure 3-31. These mixes contain 60 wt % slag, 30 wt % fly ash and 10 wt % portland cement in the premix with varying concentrations of aluminate in the SWPF simulant solution. The SWPF mixes (with the exception of GVS 125) lose less mass at 40 °C and at 60 °C curing temperatures than mixes cured at 22 °C. GVS125, which has the lowest aluminate concentration, shows a similar trend to that observed with the 45 wt % slag mixes (GVS121-GVS124).

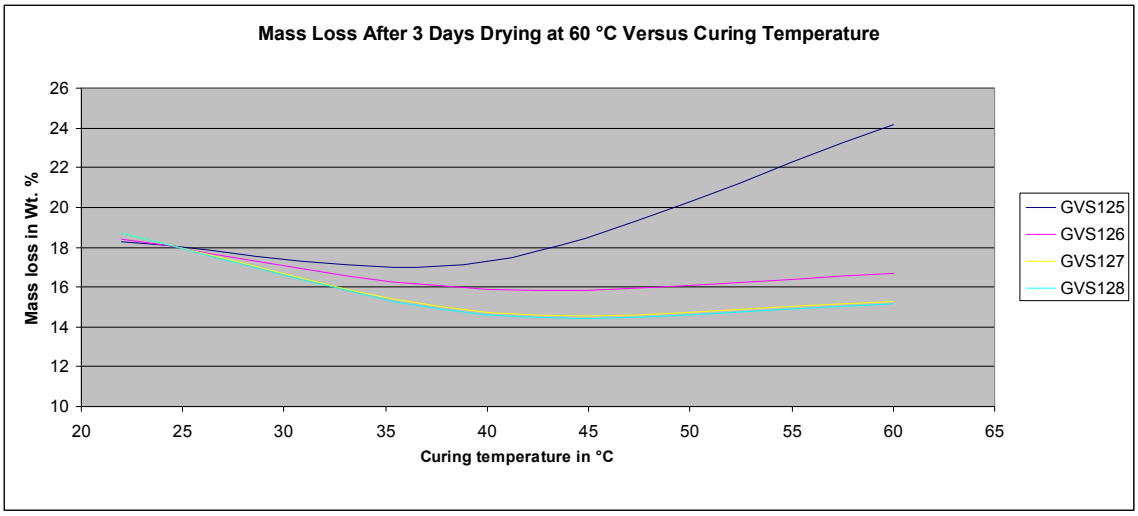

Figure 3-31. Mass loss (wt %) for GVS125-GVS128 as a function of curing temperatures after 3 days at 60 °C.

Figure 3-32 shows the mass loss as function of curing temperature for the GVS126 samples after 3 days of drying at 60 °C. These results are consistent with the mass losses in Figure 3-31. The size of the residual, saturated core after drying is roughly the same for the mixes cured 40 °C and 60 °C and larger than that observed at 22 °C. Similar results were obtained for the mixes GVS127 and GVS128. These results indicate that an increase in slag content from 45 to 60 wt % increases the performance properties for samples cured at higher temperatures. However, the aluminate concentration must be 0.45 M or greater for this to occur. Therefore, a combination of high slag content and high aluminate concentration mitigates the loss of performance for samples cured at higher temperatures.

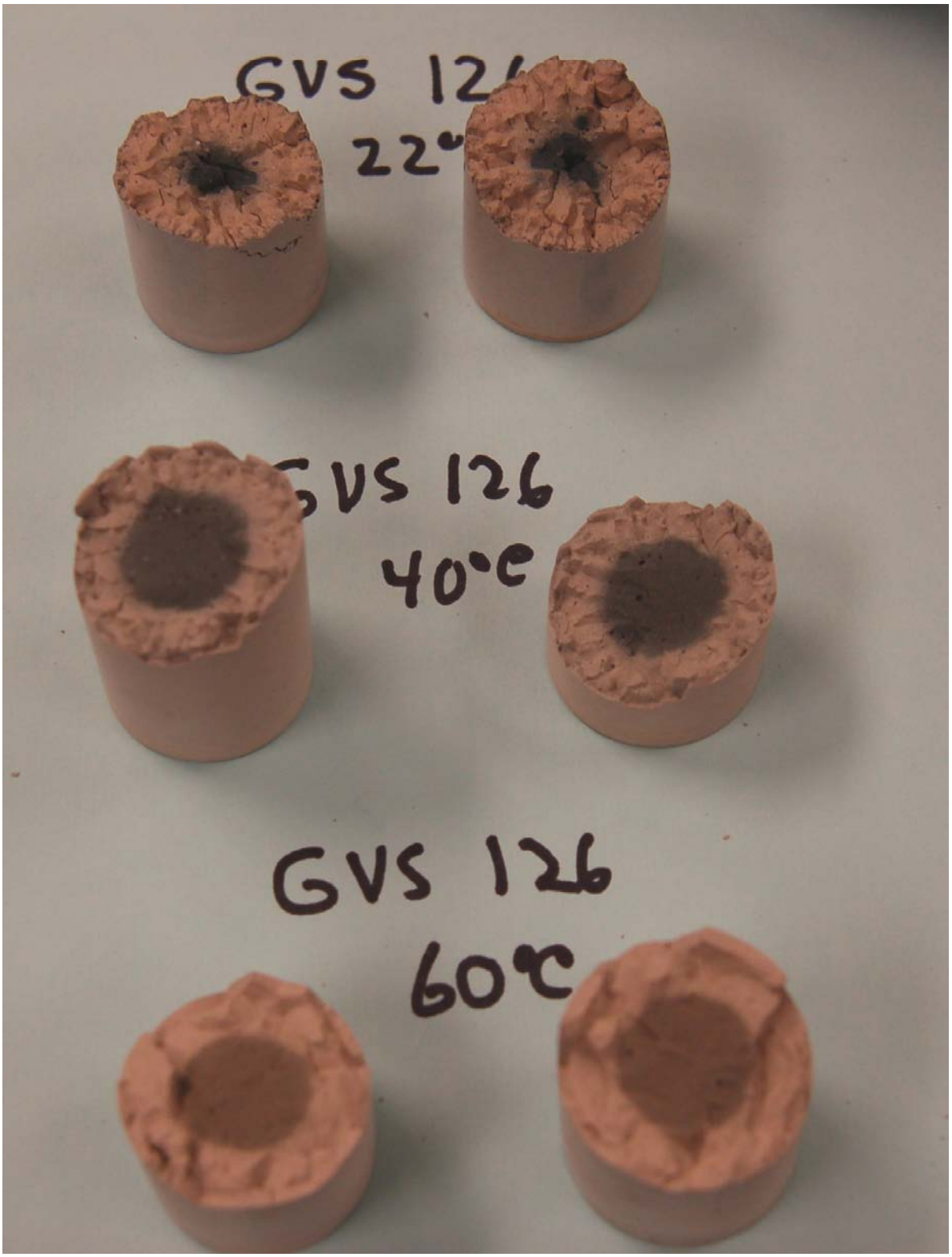

Figure 3-32. Sample GVS126 cured at 22 °C, 40 °C and 60 °C, showing higher slag content increases the performance properties at high temperatures.

4.0 PREDICTIVE MODELING FOR GROUT PROPERTIES

One of the goals of this work is to identify the factors that drive the physical properties (responses) of the Saltstone mixes. The models are developed using JMP Version 7.02 [12] for Young's modulus, heat of hydration normalized to grams of premix, heat of hydration normalized to grams of grout, plastic viscosity and yield stress. The results were obtained from samples cured at 22 °C. Although these models provide some insight into the key factors of these properties, not all of the factors were varied in the experimental design. Consequently, the models should only be applied to Phases 9 and 12 and should not be extended to general use.

For Young's modulus, the predicted versus actual values are plotted and provide a linear fit with an R^2 equal to 93% (Figure 4-1). These data points are for Phases 9 and 12 cured at 22 °C.

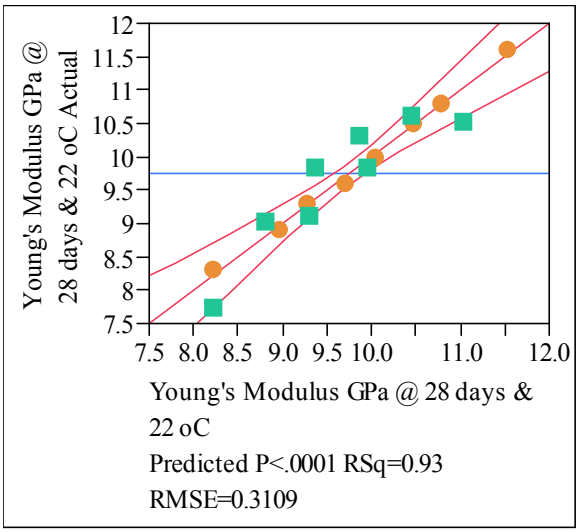

Figure 4-1. Actual versus predicted values of Young's modulus for samples of Phases 9 (●) and 12 (■) for samples cured at 22 °C.

The model for prediction of E is:

E = 17.1 – 15 • w/cm + 0.07 • wt % slag – 5.8 • aluminate molarity

The dependence of E on w/cm ratio and wt % slag is consistent with previous results for Saltstone mixes. However in the previous reports, E depended positively on aluminate concentration [9]. That is, the higher the concentration of aluminate the greater the value of E. This model shows that higher aluminate concentrations actually decrease E which is due to the aluminate concentrations of Phase 12 being extended from 0.35 M to 0.65 M. Figure 4-1 shows E decreasing as the aluminate concentrations reach these high levels which corresponds to the discussion in section 3-2.

For heat of hydration (J/g of cm), the predicted versus actual values are plotted and provide a linear fit with an R^2 equal to 98 % (Figure 4-2). These data points are for Phases 9 and 12 for the mixes cured at 22 °C.

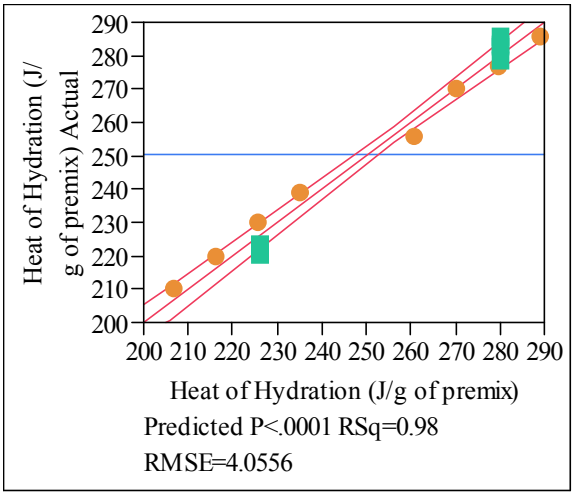

Figure 4-2. Actual vs. predicted values of heat of hydration in J/g of cementitious materials for samples of Phases 9 (●) and 12 (■).

The model for prediction of heat of hydration (HOH) expressed in J/g of cm is:

HOH = - 49.2 + 188.6 • w/cm + 3.6 • wt % slag

This model shows that increasing the slag concentration or the w/cm ratio leads to higher values of the heat of hydration (J/g of cm). Physically, this dependence on w/cm ratio is most likely due to a better dispersion of the cementitious particles within the salt solution and more water for hydration of each particle. The dependence of heat of hydration on slag content is expected since it was previously shown that the amount of heat produced from slag is higher than that produced from fly ash.

For heat of hydration (J/g of grout), the predicted versus actual values are plotted and provide a linear fit with an R^2 equal to 99% (Figure 4-3).

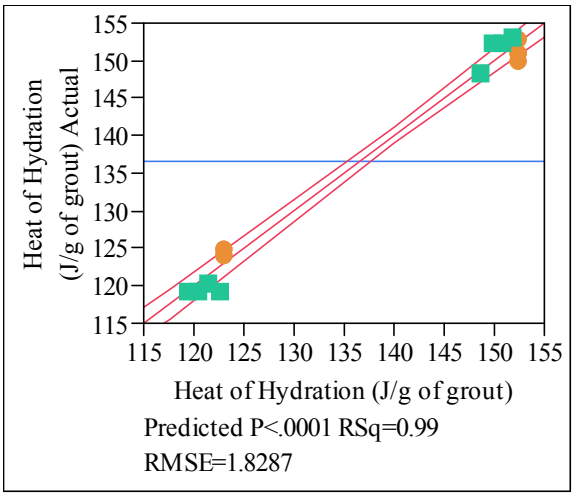

Figure 4-3. Actual vs. predicted values of heat of hydration in J/g of grout for Phases 9 (●) and 12 (■) mixes.

The model (equation) for prediction of heat of hydration (HOH) expressed in J/g of grout is:

HOH = 37.9 + 2.0 • wt % slag – 10.6 • aluminate molarity

The heat of hydration (J/g of Saltstone) reveals that w/cm ratio is not important for these Phases. This is explained by an equal balance between (1) an increase in heat of hydration (normalized to cm) with an increase in w/cm ratio and (2) a decrease in the heat of hydration (normalized to grout) as the w/cm ratio increases.

For yield stress, the predicted versus actual values are plotted and provide a linear fit with an R^2 equal to 99% (Figure 4-4).

.

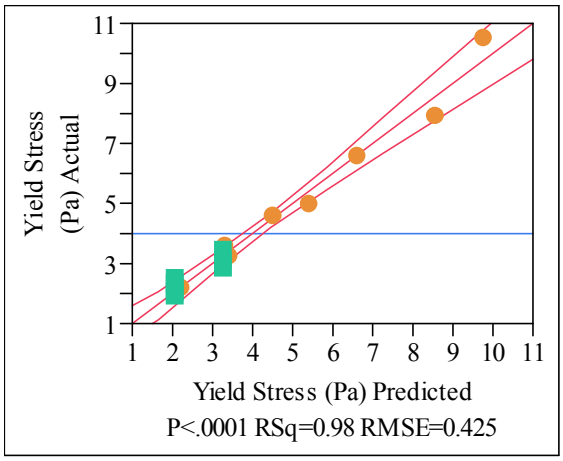

Figure 4-4. Actual versus predicted values of yield stress for samples of Phases 9 (●) and 12 (■).

The model for prediction of yield stress (Pa) is:

Yield Stress = 21.2 - 37.0 • w/cm + 0.08 • wt % slag +205 • (w/cm - 0.5875) • (w/cm - 0.5875)

In addition, the model contains a phase difference of 0.65 units between Phases 9 and 12.

In general, these results are consistent with previous results of the Variability Study [9]. An increase in w/cm ratio decreases the yield stress whereas an increase in slag concentration increases the yield stress. There is a quadratic term that gives a better fit but, plays a minor role in the overall prediction.

For plastic viscosity (mPa•s), the predicted versus actual values are plotted and provide a linear fit with an R^2 equal to 98% (Figure 4-5).

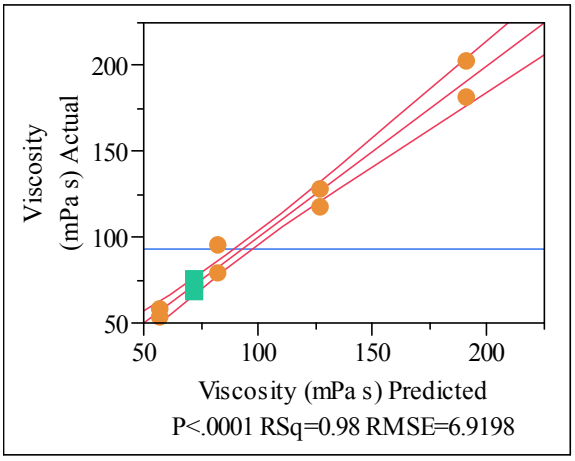

Figure 4-5. Actual vs. predicted values of viscosity for samples of Phases 9 (●) and 12 (■).

The model for prediction of plastic viscosity is:

Viscosity = 555.8 - 799 •w/cm + 3800 • (w/cm - 0.5875) • (w/cm - 0.5875)

In addition, the model contains a phase difference of 5.7 units between Phases 9 and 12.

The plastic viscosity depends mainly on w/cm ratio as expected where higher w/cm ratios lead to lower viscosity. As with the yield stress model, there is a quadratic term that gives a better fit but, plays a minor role in the overall prediction.

5.0 CONCLUSIONS

Task 4 of the FY09 Variability Study focused mainly on the performance properties of Saltstone mixes batched using the projected SWPF salt solution but with varying aluminate concentrations. The major conclusions of this task are provided in this Section.

The key factors that drive performance of the SWPF mixes were determined to be (1) the time/temperature profile for curing, (2) water to cementitious materials ratio, (3) aluminate concentration in the waste stream, and (4) wt % slag in the premix.

An increase in the curing temperature for mixes with 45 wt % slag results in a large decrease in Young's modulus. However, for mixes containing 60 wt % slag, only a small decrease in Young's modulus was observed between mixes cured at 22 °C and 60 °C. The importance of curing conditions can therefore, not be overemphasized. The gain realized in performance by, e.g., a higher level of aluminate or wt % slag or a reduction in w/cm ratio, can be offset by a higher curing temperature. The reduction in performance at higher curing temperatures is consistent with results obtained in a separate study which, although preliminary, showed that curing a Saltstone mix at 60 °C increased the hydraulic conductivity by several orders of magnitude. Control of the time/temperature curing profile can be managed by pour schedules and other temperature control measures.

An increase in dynamic Young's modulus (indicator of performance) is observed as the w/cm ratio decreases. The w/cm ratio is a process parameter which can be adjusted to improve performance as long as the processing properties of the grout are still within an operational window that will lead to successful placement. The same conclusions apply to wt % slag in the premix. That is, an increase in the wt % slag at the expense of fly ash in the premix increases Young's modulus and performance.

The performance properties of SWPF mixes show a non-linear dependence on aluminate concentration. As the aluminate concentration is increased from 0.1 M to 0.25 M, the Young's modulus and compressive strength increase and the total porosity is reduced. In the region of 0.25 to 0.45 M aluminate, very little change is observed in any of the properties. However, a further increase in the aluminate concentration from 0.45 M to 0.65 M leads to a reduction in Young's modulus. The processing properties also follow this non-linear response with the set time reduced from 3 days to 1 day at the highest aluminate levels. This non-linear response of both performance and processing properties to aluminate concentration indicates that the waste stream may need to be carefully monitored for aluminate.

A simple method was developed as part of this task that reveals general trends in permeability and microstructure of the cured grout samples as a function of curing temperature. This method reveals that curing at higher temperatures (e.g., 60 °C) results in a higher permeability as well as a different microstructure than the microstructure observed for the same mixes cured at 22 °C. Measurements of the heat of hydration at 50 °C reveal that in mixes with aluminate

concentrations >0.25 M, the degree of hydration is also reduced by curing at higher temperatures.

Linear, empirical models were developed and are presented in this report for Young's modulus, heat of hydration normalized to the mass of premix, heat of hydration normalized to the mass of grout, yield stress and plastic viscosity. The models included only data from the mixes batched as part of Phases 9 and 12. Therefore, the models quantify the statistically significant factors that drive the performance and processing properties over the ranges selected in the designs for Phases 9 and 12. The R^2 values for these three models ranged from 93% to 99%.

The final performance properties of SWPF mixes are dependent upon a number of interactive factors in a complex fashion. Depending upon the values of the performance properties that are required to meet the Performance Assessment, these factors may need to be controlled to get to the desired outcome.

6.0 PATH FORWARD

The reduction in performance properties for mixes cured at higher temperatures remains a significant issue. Additional measurements of heat of hydration at higher isothermal temperatures are recommended to determine the role of degree of hydration in this observed reduction in performance. The microstructural changes that occur at higher curing temperatures should also be investigated by scanning electron microscopy and other methods. Finally, actual measurements of permeability as a function of curing temperature should be carried out.

7.0 REFERENCES

[1] *Memo Report on the Subtasks for the Saltstone Variability Study for 2009*, J. R. Harbour and T. B. Edwards, SRNL L3100-2008-00048, October 2008.

[2] *Effect of Increased Aluminate Concentrations on Saltstone Mixes,* J. R. Harbour, T. B. Edwards, E. K. Hansen and V. J. Williams, WSRC-STI-2007-00506, Rev. 0, 2007.

[3] *Report in progress*, K. L. Dixon, J. R. Harbour and M. A. Phifer, 2010.

[4] *Impact of Time/Temperature Curing Conditions and Aluminate Concentration on Saltstone Properties,* J. R. Harbour, T. B. Edwards and V. J. Williams, SRNL-STI-2009-00184, Rev. 0, 2009.

[5] *Heat of Hydration of Saltstone Mixes – Measurement by Isothermal Calorimetry*, J. R. Harbour, V. J. Williams and T. B. Edwards, WSRC-STI-2007-00263, Rev. 0, 2007.

[6] *Saltstone Performance Indicator*, J. R. Harbour and V. J. Williams, SRNL-STI-2008-00488, Rev. 0, December 2008.

[7] *Saltstone Variability Study –Measurement of Porosity,* J.R. Harbour, V.J. Williams, T.B. Edwards, R.E. Eibling, and R.F. Schumacher, WSRC-STI-2007-00352, Rev. 0.

[8] *Variability Study for Saltstone*, J. R. Harbour, T. B. Edwards, E. K. Hansen and V. J. Williams, WSRC-TR-2005-00447, October 2005.

[9] *Impact of Time/Temperature Curing Conditions and Aluminate Concentration on Saltstone Properties,* J. R. Harbour, T. B. Edwards and V. J. Williams, SRNL-STI-2009-00184, Rev. 0.

[10] *Key Factors that influence the Performance Properties of ARP/MCU Saltstone Mixes,* J. R. Harbour, T. B. Edwards, and V. J. Williams, SRNL-STI-2009-00546, Rev. 0, 2009.

[11] *Cement Chemistry*, H. R. W. Taylor, Thomas Telford Publishing, 1997.

[12] JMP Version 7.0.2, SAS Institute, Inc. Cary, NC, 1989-2007.